

UCSF

UC San Francisco Previously Published Works

Title

Diethylstilbestrol-induced mouse hypospadias: “window of susceptibility”

Permalink

<https://escholarship.org/uc/item/1qx2n8n0>

Journal

Differentiation, 91(1-3)

ISSN

0301-4681

Authors

Sinclair, Adriane Watkins

Cao, Mei

Baskin, Laurence

et al.

Publication Date

2016

DOI

10.1016/j.diff.2016.01.004

Peer reviewed

Dear Author,

Please, note that changes made to the HTML content will be added to the article before publication, but are not reflected in this PDF.

Note also that this file should not be used for submitting corrections.



Contents lists available at ScienceDirect

Differentiation

journal homepage: www.elsevier.com/locate/diff

Review article

Diethylstilbestrol-induced mouse hypospadias: “window of susceptibility”

Q1 Adriane Watkins Sinclair^a, Mei Cao^a, Laurence Baskin^a, Gerald R. Cunha^{a,*}

^a Department of Urology, University of California San Francisco, 400 Parnassus Avenue, Box A610, San Francisco, CA 94143, United States

ARTICLE INFO

Article history:

Received 14 November 2015

Accepted 7 January 2016

Keywords:

Diethylstilbestrol

Estrogen

Mouse penile development

Urethra

ABSTRACT

Q2 Hypospadias, an abnormality affecting the penile urethra, is one of the most prevalent congenital malformations afflicting human males. The morphology of hypospadias is markedly different in humans versus mice reflecting substantial differences in penile development in humans and mice. Estrogens such as diethylstilbestrol (DES) elicit mouse penile malformations, but the types of penile abnormalities differ depending on whether DES treatment is prenatal or neonatal. To define the actual “window of susceptibility” to the adverse effects of DES, pregnant mice and their neonatal pups were injected subcutaneously with 200ng/gbw DES every other day from embryonic day 12–18 (DES E12–E18), postnatal day 0–10 (DES P0–P10), embryonic day 12 to postnatal day 10 (DES E12–P10), postnatal day 5–15 (DES P5–P15), and postnatal day 10–20 (DES P10–P20). Aged-matched controls received sesame oil vehicle. After euthanasia at 10, 15, 20 and 60 days, penises were analyzed by gross morphology, histology and morphometry. Penises of all 5 groups of DES-treated mice were reduced in size, which was confirmed by morphometric analysis of internal penile structures. The most profound effects were seen in the DES E12–P10, DES P0–P10, and DES P5–P15 groups, thus defining a DES “programming window”. For all parameters, DES treatment from P10 to P20 showed the most mild of effects. Adverse effects of DES on the MUMP cartilage and erectile bodies observed shortly after the last DES injection reverted to normality in the DES P5–P15, but not in the E12–P10 and P0–P10 groups, in which MUMP cartilage and erectile body malformations persisted into adulthood, again emphasizing a “window of susceptibility” in the early neonatal period.

© 2016 Published by Elsevier B.V. on behalf of International Society of Differentiation

Contents

1. Introduction	2
2. Materials and methods	5
2.1. Animals	5
2.2. Hormonal treatments	5
2.3. Specimen preparation and analysis	5
2.4. Scanning electron microscopy	6
2.5. Morphometric analysis	7
2.6. Statistics	8
3. Results	8
3.1. Morphometric analysis	10
3.1.1. Prenatal DES (E12–E18) analyzed on day P10	11
3.1.2. Pre+Postnatal DES E12–P10 analyzed on day P10	11
3.1.3. Postnatal DES (P0–P10 and P5–P15) analyzed on day P10 and day P15	11
3.1.4. Postnatal DES (P10–P20) analyzed on day 20	12
3.2. Normalization of morphometric data	12
3.3. Effect of DES on differentiation of the MUMP cartilage and erectile bodies	13
4. Discussion	14

Abbreviations: DES, Diethylstilbestrol; E, embryonic; P, postnatal

* Corresponding author.

E-mail address: gerald.cunha@ucsf.edu (G.R. Cunha).

<http://dx.doi.org/10.1016/j.diff.2016.01.004>

Join the International Society for Differentiation (www.isdifferentiation.org)

0301-4681/© 2016 Published by Elsevier B.V. on behalf of International Society of Differentiation

Acknowledgments.....	18	67
References.....	18	68

1. Introduction

Hypospadias is the second most common urogenital anomaly in boys occurring in approximately 1:200–1:300 male births (Baskin, 2000), and the incidence of this congenital defect in the USA has doubled in recent times (Paulozzi et al., 1997; Paulozzi, 1999). The etiology of hypospadias in the majority of patients remains undefined, but is thought to involve both genetic susceptibility and environmental exposure to endocrine disruptors (West and Brenner, 1985; Baskin and Ebberts, 2006; Willingham and Baskin, 2007; Wang and Baskin, 2008; Kalfa et al., 2011). Treatment of hypospadias remains surgical, and multiple surgeries are often required for a functional and a cosmetically acceptable reconstruction (Lee et al., 2013). Patients with severe hypospadias are at risk for surgical complications that can lead to life long difficulties with urination, sexual function and psychological problems. Thus, hypospadias is a significant medical condition that consumes substantial health care resources.

An alternative approach to ameliorating hypospadias is prevention. If a genetically at-risk cohort could be identified and potentially causative environmental agents (endocrine disruptors) avoided, then the incidence of hypospadias could be reduced (Baskin et al., 2001a; Willingham and Baskin, 2007). For example, the incidence of hypospadias has been shown to be increased in families undergoing in vitro fertilization (Nordenvall et al., 2013), perhaps because progesterone is administered to maintain receptivity of uterus to the embryo. Progestins have been implicated as a potential cause of hypospadias in both animal and human studies (Carmichael et al., 2005; Willingham et al., 2006a; Agras et al., 2007). Animal models of hypospadias have demonstrated a causal relationship between hypospadias and prenatal exposure to a variety of agents: estrogens, progesterone, Loratidine, “androgen blockers” (flutamide, finasteride, anti-androgenic fungicides [vinclozolin and procymidone], and phthalates) (Clark et al., 1993; Ostby et al., 1999; Kojima et al., 2002; Kim et al., 2004; Carmichael et al., 2005; Foster and Harris, 2005; Buckley et al., 2006; Willingham et al., 2006b; Ormond et al., 2009; Rider et al., 2009). The persistent question concerns the relevance of animal models to human hypospadias (Cunha et al., 2015b).

Estrogens are known to induce hypospadias in mice, and many studies use diethylstilbestrol (DES) as the teratogenic agent. The types of penile malformations seen in mice differ depending on whether DES treatment is prenatal or neonatal (Kim et al., 2004; Mahawong et al., 2014b, 2014a). It is likely, however, that a wider age range of DES exposure would reveal the “window of susceptibility” to adverse effects of DES, before and after which DES treatment may be without long-term teratogenic effects on individual elements within the developing external genitalia. Moreover, a thorough investigation of the effects of DES over a wide age range of treatment may (a) elucidate the morphogenetic mechanisms involved in generating abnormal penile morphology and hypospadias and (b) reveal those penile elements more (or less) sensitive on a temporal basis to developmental exposure to DES. Such an approach may also explain why certain effects of DES elicited and expressed during development resolve to normality in adulthood (Cunha et al., 2015b).

Hypospadias results from perturbation of normal penile development (Baskin et al., 1998), and thus can only be understood in the context of normal development of the penis, a complex organ with a precise anatomical patterning of its individual

internal components. In humans, hypospadias refers to three related anomalies: (a) a urethral defect, (b) a preputial defect and (c) chordee (abnormal curvature of the penis). The abnormal urethral orifice may be situated distally in the glans, at mid-shaft, or in the perineum, indicative of mild, moderate or severe hypospadias (Cunha et al., 2015b). Associated with the defect in the urethral meatus is absence or hypoplasia of the corpus spongiosum as well as absence of the ventral aspect of the prepuce (Baskin et al., 1998).

Substantial differences in anatomy and development of the human versus the mouse penis necessarily translate to profound differences in the nature of hypospadias in these two species (Cunha et al., 2015b). In a general sense, hypospadias represents a perturbation of patterning of the elements constituting the penis, especially the positioning of the urethral meatus. While the various forms of human hypospadias are obvious on physical examination, hypospadias in the mouse is more subtle. First of all mouse hypospadias does not involve “mid-shaft” malformations similar to that in humans. Indeed, prenatally estrogen-induced mouse hypospadias is characterized by subtle alteration in the (a) patterning of elements constituting the urethral meatus, namely the male urogenital mating protuberance (MUMP) and MUMP ridge, (b) an altered positioning of internal penile elements such as the os penis and urethral flaps relative to the urethral meatus and (c) malformation of the corpus cavernosum urethrae, the homolog of the human corpus spongiosum (Cunha et al., 2015b) (urethral flaps are projections of the corpora cavernosa urethrae into the urethral lumen) (Rodriguez et al., 2011). Even though mouse and human hypospadias are distinctly different, estrogen-induced mouse hypospadias exhibits certain morphogenetic homologies to human hypospadias based upon developmental processes common to both species (Mahawong et al., 2014b, 2014a; Cunha et al., 2015b). Whether penile defects elicited in mice by other agents (“androgen blockers” such as anti-androgen or 5 α -reductase inhibitors, progesterone, phthalates, etc.) generate mid-shaft hypospadias remains to be seen.

Initial development of external genitalia in human and mouse embryos occurs identically in males and females and results in formation of the midline ambisexual genital tubercle, which is the primordium of the penis in males and the clitoris in females. In males, fetal testicular androgens elicit elongation of the genital tubercle. In both humans and mice a solid epithelial urethral plate forms (Fig. 1) that extends distally towards the tip of the genital tubercle. However, subsequent development of the urethral plate is radically different in humans versus mice. In humans, the urethral plate canalizes to form a wide urethral groove bounded laterally by urethral folds (Figs. 2, 3A, 5A and B) (Li et al., 2014). The human penile urethra forms as a result of midline fusion of the urethral folds, a process that begins proximally in the perineum and extends distally towards the glans penis (Figs. 2, 3, 4, 5A–C) (Li et al., 2014). Canalization of the urethral plate to form the urethral groove and subsequent fusion of the urethral folds to form the tubular urethra is particularly well illustrated in scanning electron micrographs (Fig. 3).

In mice the embryonic urethral plate extends to near the distal aspect of the genital tubercle, and canalizes to directly form most of the penile urethra (Fig. 5 D–F) (Hynes and Fraher, 2004a; Seifert et al., 2008). However, by birth the murine urethral plate is no longer observed within the distal aspect of the genital tubercle (Fig. 6A). Instead a ventral groove forms whose edges

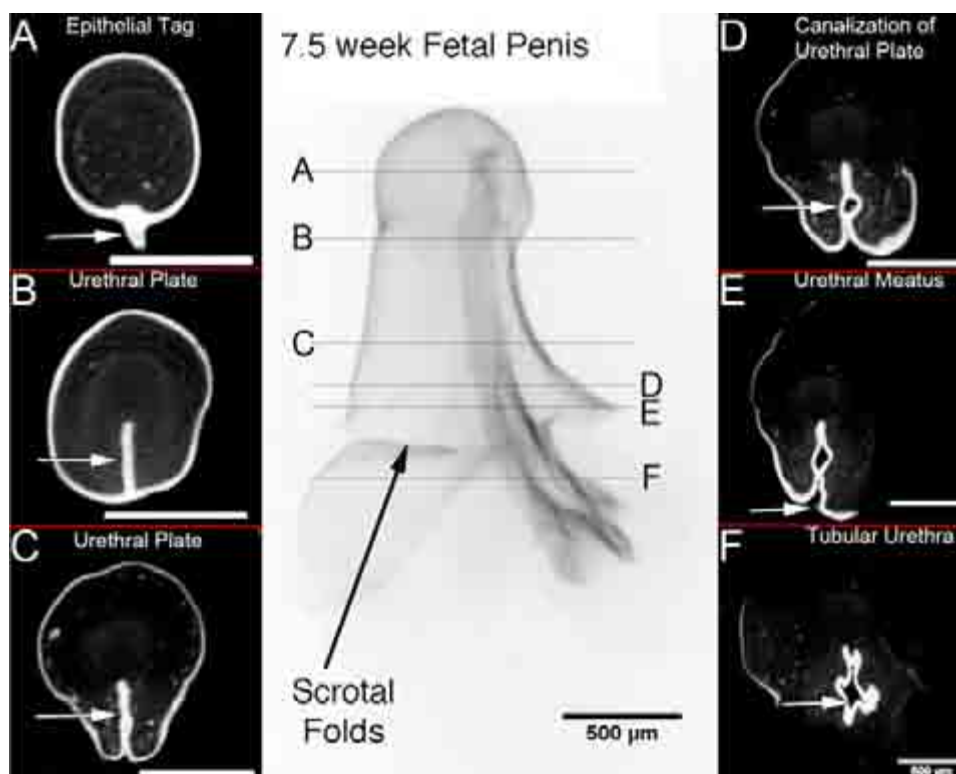


Fig. 1. Optical Projection Tomography of a 7.5 week human fetal penis at the indifferent stage of development. The epithelium is stained for E-Cadherin. Histologic sections A–F correspond to the horizontal lines in the gross OPT specimen. Note the epithelial tag in A (arrow), the urethral plate in B (arrow), canalization of the urethral plate in C and D (arrow), the urethral groove in D, the urethral meatus in E and the tubular urethral in F (white arrows). Adapted from Li et al. (2014) with permission.

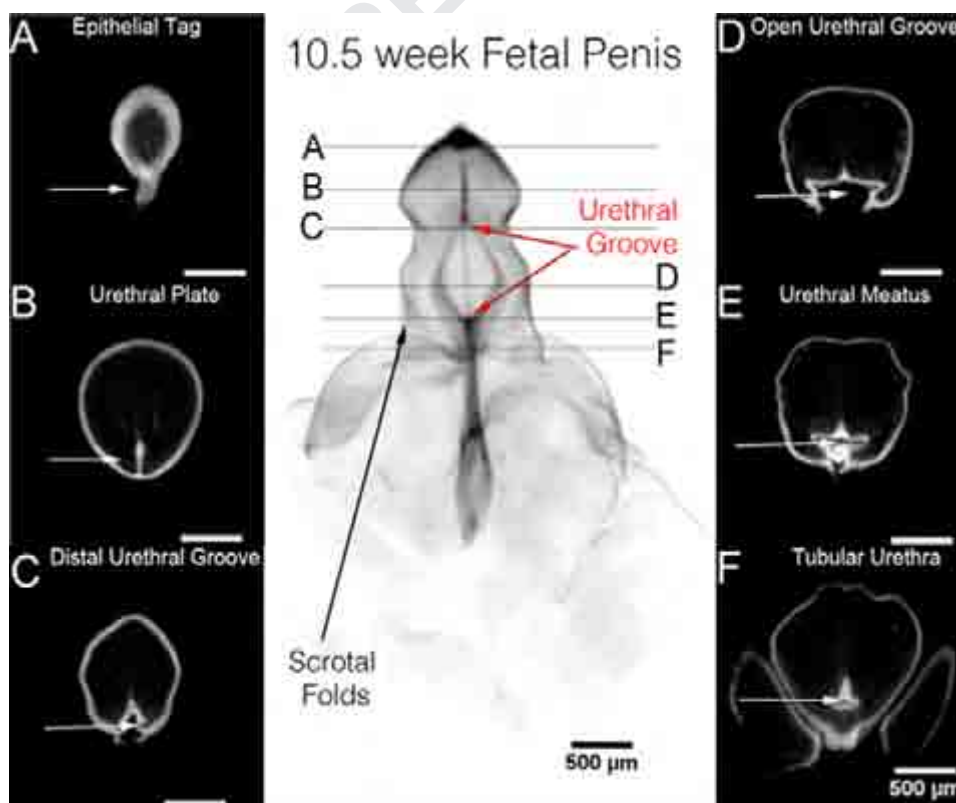


Fig. 2. Optical Projection Tomography (OPT) of a 10.5 week human fetal penis. The epithelium is stained for E-Cadherin. OPT sections A–F correspond to the horizontal lines in the gross OPT specimen. Note the epithelial tag in A, the urethral plate in B within the glans, the distal urethral groove in C, the urethral groove in D, the urethral meatus in E and the tubular urethral in F (white arrows). Adapted from Li et al. (2014) with permission.

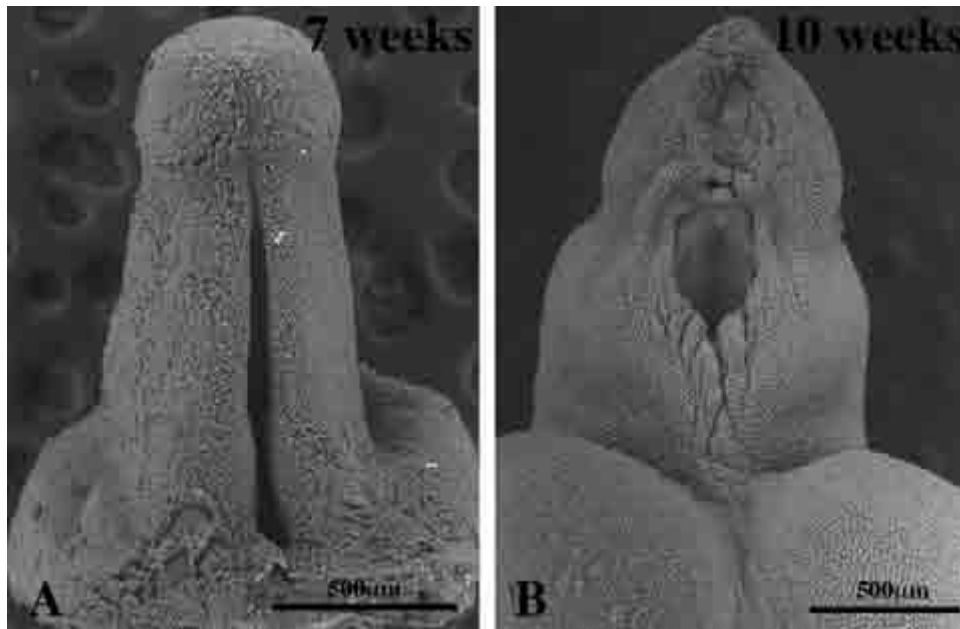


Fig. 3. Scanning electron micrographs of human fetal penises at 7 and 10 weeks of gestation. In (A) note the prominent urethral groove. In (B) the edges of the urethral groove are fusing in the midline to form the urethra, but the distal urethral groove is still widely open.

subsequently fuse to form the distal aspect of the mouse penile urethra and especially the urethral meatus (Fig. 5G–I and 6) (Mahawong et al., 2014a). Several lines of evidence support the notion that the mouse urethral meatus forms via multiple fusion events (Yang et al., 2010; Rodriguez et al., 2011; Blaschko et al., 2013; Mahawong et al., 2014b, 2014a). Fig. 5 illustrates the differences in the fate of the urethral plate in humans versus mice.

The proposed mechanism for development of human

hypospadias is failure of formation or fusion of the urethral folds, with the site of failure of urethral fold fusion dictating the position of the abnormal urethral meatus (Hutson et al., 2014; Cunha et al., 2015a). In mice this morphogenetic mechanism most certainly does not apply to that region of the mouse penile urethra which forms directly from canalization of the urethral plate, but appears to be applicable to formation of the distal aspect of the murine urethra and the urethral meatus that forms as a result of epithelial

Development of the Human Male Urethra

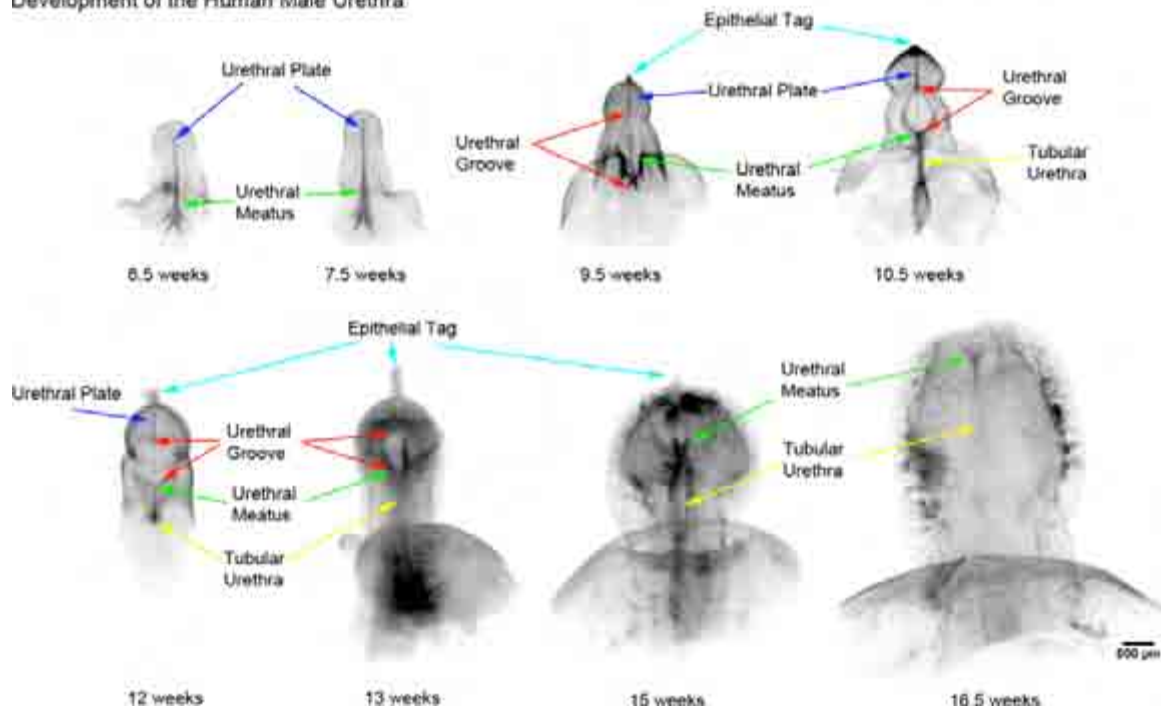


Fig. 4. Optical Projection Tomography of male penile urethral development from 6.5 weeks to 16.5 weeks of gestation. Note the progression of the penile urethral meatus (green arrows) from the scrotal folds at 6.5 weeks to a terminal position on the glans at 16.5 weeks. The open urethral groove (red arrows) is best seen from 9.5 to 13 weeks with clear progression of a proximal to distal fusion of the edges of urethral groove to form the tubular urethra (yellow arrows). At 13 weeks the urethra groove is within the glans penis with the tubular urethra completely formed within the shaft of the penis consistent with the endodermal theory of urethral development. Adapted from Li et al. (2014) with permission. (For interpretation of the references to color in this figure legend, the reader is referred to the web version of this article.)

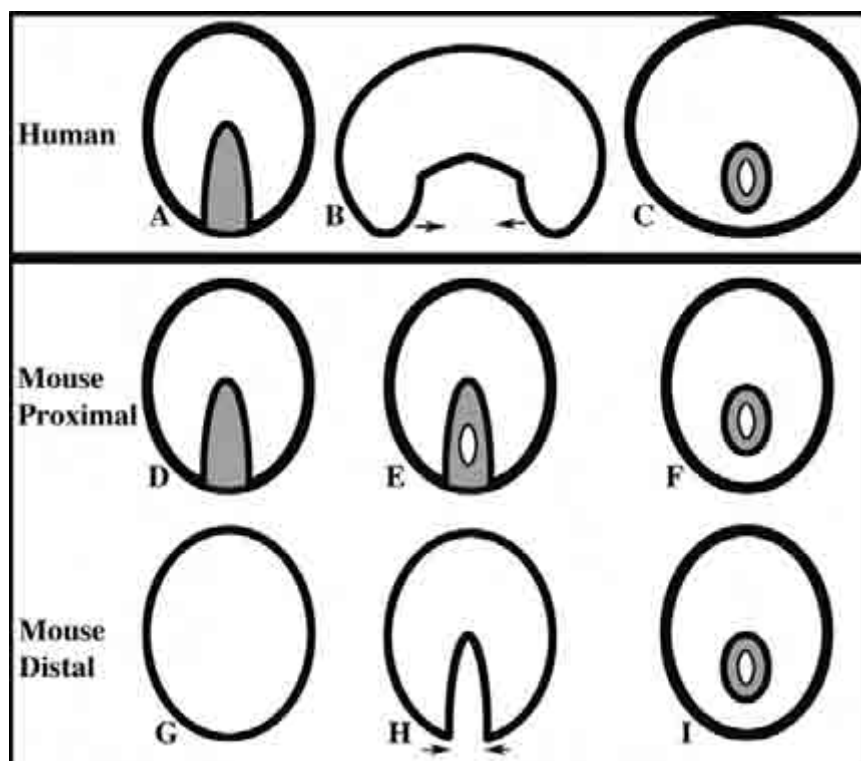


Fig. 5. Comparison of human and mouse penile urethral development. In humans the urethral plate (A, shaded) canalizes to form a wide urethral groove (B), whose edges subsequently fuse in the midline to form the penile urethra (C). In mice, the urethral plate (D, shaded) canalizes to directly form most of the penile urethra (E and F) as described (Hynes and Fraher, 2004a, 2004b; Seifert et al., 2008). As development proceeds, the distal aspect of the newborn mouse genital tubercle is devoid of urethral plate (G). In this region a ventral groove forms (H) whose edges subsequently fuse to form the distal aspect of the mouse penile urethra (I).

fusion events as discussed above.

Estrogens are one type of agent known to induce penile malformations in mice, and especially malformations of the urethral meatus interpreted as hypospadias. Estrogen-induced penile malformations observed in adulthood surely have developmental correlates, which need to be explored to reveal teratogenic mechanisms. In this regard, an excellent method to validate DES-induced alterations during development is morphometric analysis, which builds on our previous morphometric analysis of normal mouse penile development as the baseline (Schlomer et al., 2013). As reported previously, prenatal and neonatal DES treatment severely reduces size of the mouse penis when examined during the neonatal period (Mahawong et al., 2014b, 2014a), an effect that persists into adulthood. Consequently, morphometric analysis of developmental effects of DES must take into account the overall global reduction in size of the external genitalia. Our past papers have demonstrated differences in the incidence and spectrum of malformations depending on whether DES is administered prenatally (E12-E18) versus neonatally (P0-P10) to mice. The current study, utilizing a broader range of treatment periods, is designed to define the “window of susceptibility” to the adverse developmental effects of DES and to determine those malformations seen immediately after termination of DES treatment that either lead to enduring adult penile malformations or revert to normality by adulthood.

2. Materials and methods

2.1. Animals

Animal care and research protocols were approved by the Animal Care and Use Committee of the University of California, San

Francisco (UCSF). Adult wild-type CD-1 mice (Charles River Breeding Laboratories, Wilmington, MA, USA) and their offspring were housed in polycarbonate cages (20 × 25 × 47 cm³) with laboratory grade pellet bedding in the UCSF Pathogen Specific Barrier facility. Mice were given water *ad libitum* and fed LabDiet 5058 (PMI Nutrition International, P. O. Box 66812, St. Louis, MO 63166), whose content of phytoestrogen is incapable of eliciting vaginal cornification in ovariectomized adult mice (Buchanan et al., 1998).

2.2. Hormonal treatments

Pregnant CD-1 dams were weighed and injected subcutaneously on days 12, 14, 16, and 18 of gestation with DES at a concentration of 200ng/g body weight in ~5 μl sesame oil vehicle. Control group dams were injected with 5 μl sesame oil. Separate Hamilton syringes were used for sesame oil and DES. For postnatal DES treatment, the day of birth was counted as day 0, and pups were weighed and injected subcutaneously with either DES (200 ng /gwb) or oil (5 μl) on days 1, 3, 5, 7, 9 (P0-P10 & E12-P10), on days 5, 7, 9, 11, 13 (P5-P15) or on days 10, 12, 14, 16, 18 (P10-P20).

2.3. Specimen preparation and analysis

DES- or oil-treated CD-1 mice were euthanized at the postnatal ages specified in Table 1. Sex was confirmed by gonadal inspection, and the external genitalia were dissected and fixed in 10% buffered formalin for a minimum of 24 h. Specimens were decalcified using 0.2 mM EDTA pH 6.6 for 4–6 days depending on the tissue size, embedded in paraffin and serially sectioned at 7 μm for histological staining with hematoxylin and eosin.

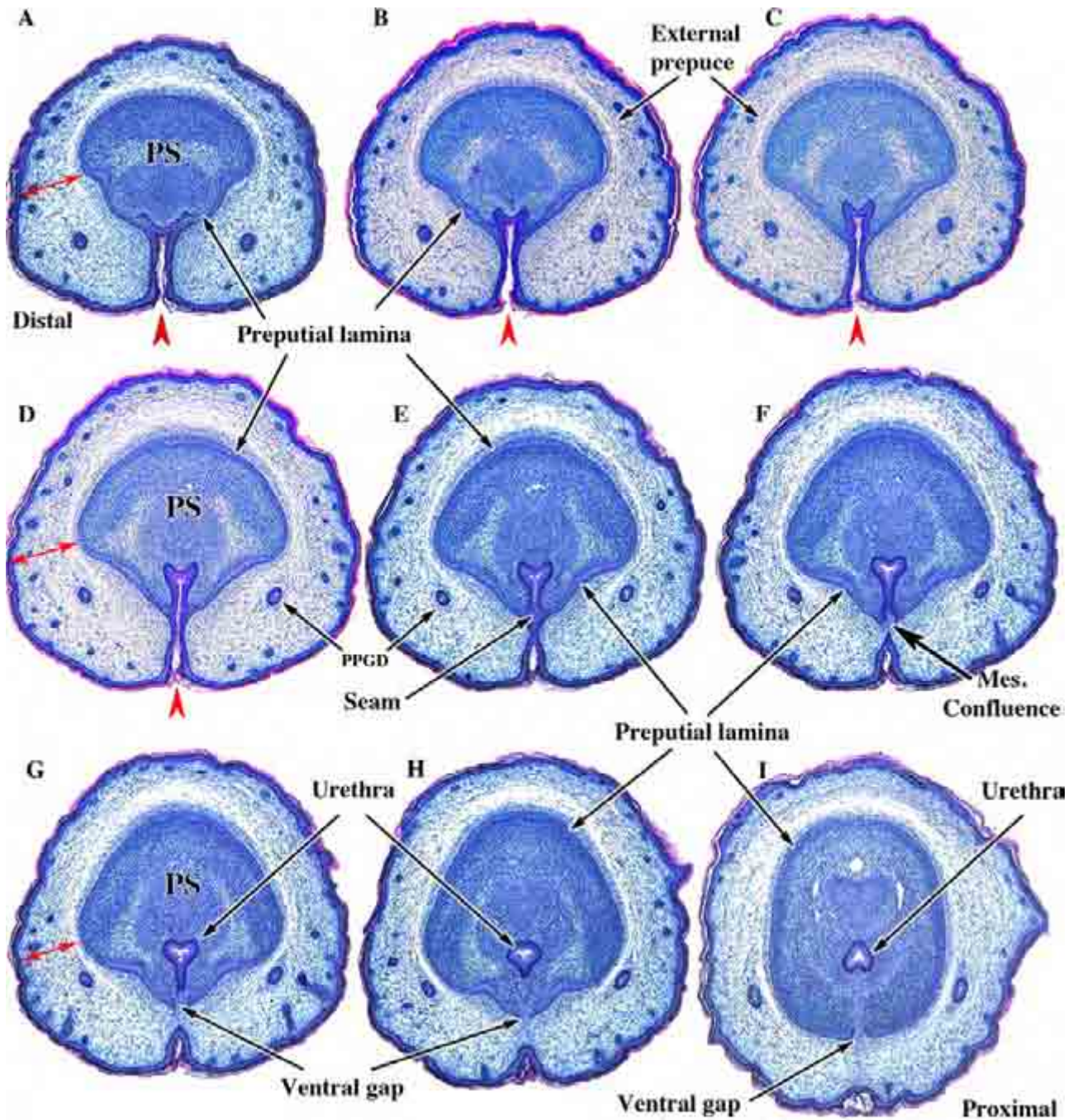


Fig. 6. Transverse sections of newborn male CD-1 external genitalia. Sections are arranged from distal (A) to proximal (I). In (A) note the thick wall of the prepuce (double-headed red arrows) containing the preputial gland ducts (PPGD). The developing penis at this distal location consists of dense penile stroma (PS) surrounded by epithelium of the preputial lamina. Note the open ventral cleft (red arrow heads) and the absence of a solid urethral plate and tubular urethra in (A–D). In (E), a slightly more proximal section, note that the ventral cleft has become subdivided into a tubular urethra dorsally via midline fusion of epithelial layers to create a midline epithelial seam. The tubular urethra thus formed now lies within penile stroma encompassed by the preputial lamina, but the epithelium of the tubular urethra is attached to the preputial lamina (E & F). In (F) note that the epithelial seam has disappeared with mesenchymal confluence across the midline. As the urethral epithelium becomes detached from the preputial lamina (G–I), a ventral gap appears in the preputial lamina (G–I). The mesenchyme-filled ventral gap in the preputial lamina represents confluence between penile stroma and preputial stroma. Adapted from Mahawang et al. 2014a with permission. (For interpretation of the references to color in this figure legend, the reader is referred to the web version of this article.)

2.4. Scanning electron microscopy

Surface details of human fetal penises were elucidated using scanning electron microscopy (SEM). Human fetal penises were obtained from abortus specimens without patient identifiers (UCSF IRB 12-08813). Age of the specimens (7 and 10 weeks of

gestation) was determined by heel-toe measurement (Taguchi et al., 1983; Drey et al., 2005). After dissection the specimens were fixed in 2% glutaraldehyde in 0.1 M sodium cacodylate buffer at pH 7.2 for 6 h, post-fixed in 2% osmium tetroxide for 2 h, dehydrated in serial alcohol solutions and critical point dried in a Tousimis AutoSamdri 815 Critical Point Dryer (Tousimis, Rockville, MD). The

Table 1
Treatment groups and age of analysis.

Treatment group	Treatment period	Age at harvest
Prenatal DES	E12-E18	P10 (N=6), P60 (N=10)
Postnatal DES 0-10	P0-P10	P10 (N=8), P60 (N=12)
Prenatal + Postnatal DES	E12-P10	E10 (N=6), P60 (N=6)
Postnatal DES 5-15	P5-P15	P15 (N=8), P60 (N=7)
Postnatal DES 10-20	P10-P20	P20 (N=7), P60 (N=7)
Oil	All of the above groups	P10 (N=21), P15 (N=8), P20 (N=7), P60 (N=39)

E=embryonic, P=postnatal.

samples were then mounted on a stub with carbon tape, and

images were obtained using a Hitachi TM-1000 Scanning Electron Microscope (Hitachi High Technologies America, Inc. Pleasanton, CA).

2.5. Morphometric analysis

Metrics of pertinent key penile morphological features (Fig. 3) were obtained by counting the number of serial histologic sections from the distal tip of the developing penis (the distal tip of the dorsal mesenchymal columns) to the beginning of the morphologic feature of interest as described previously (Schlomer et al., 2013). Since several features are bilateral (dorsal, lateral and ventral mesenchymal columns) and since perfect vertical orientation of the specimen in the paraffin block is not always

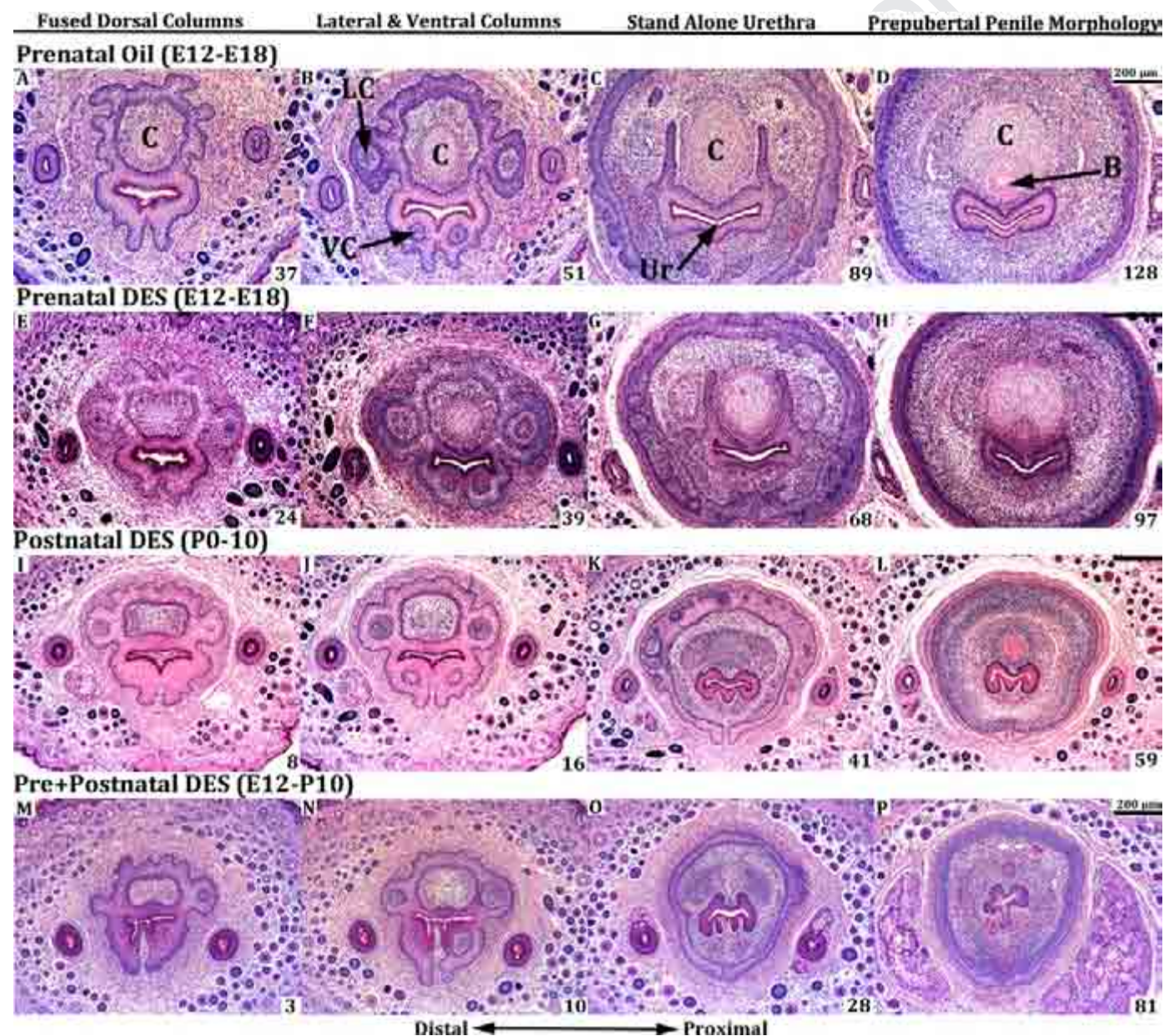


Fig. 7. Transverse serial sections of 10-day-old CD1 mouse penises treated with oil or DES (Oil, DES E13-E18, DES P0-P10 and DES E12-P10). Sections proceed from distal to proximal (left to right). Section (D) represents normal prepubertal penile morphology in which the penis is defined circumferentially by the external preputial lamina and contains a stand-alone urethra (Ur), os penis (B) and MUMP cartilage (C). Note the smaller penile diameter (defined by the preputial lamina) of the DES P0-P10 and DES E12-P10 groups as compared to oil control. A DES effect on penile length is also evident. Note that the distance from A to D in the oil treated group spans 91 (7 μm) sections, whereas this distance is reduced to 73 sections in the DES E12-E18 group, to 51 sections in the DES P0-P10 group, and to 78 sections in the DES PE12-P10 group, suggesting a smaller overall penile size in the DES-treated groups. The lack of developing MUMP cartilage (I, J, M, N) and impaired development of the MUMP corpus cavernosum (K, L, O, P) is visible in the DES P0-10 and DES E12-P10 groups. All images are at the same magnification. LC=lateral mesenchymal column, VC=ventral mesenchymal column.

possible, right and left features may appear in different, but closely associated sections. In this case, section numbers for the right and left elements were averaged to give the start point for each element pair.

2.6. Statistics

Comparison of morphological measures was done using either

student's *T* tests, or ANOVA with Bonferroni correction. A *p* value < 0.05 was considered significant. A *p* value of ≤ 0.05 is represented by †, $p \leq 0.001$ by ◆, and $p \leq 0.0001$ by ★.

3. Results

Serial histologic sections were used to determine the effects of

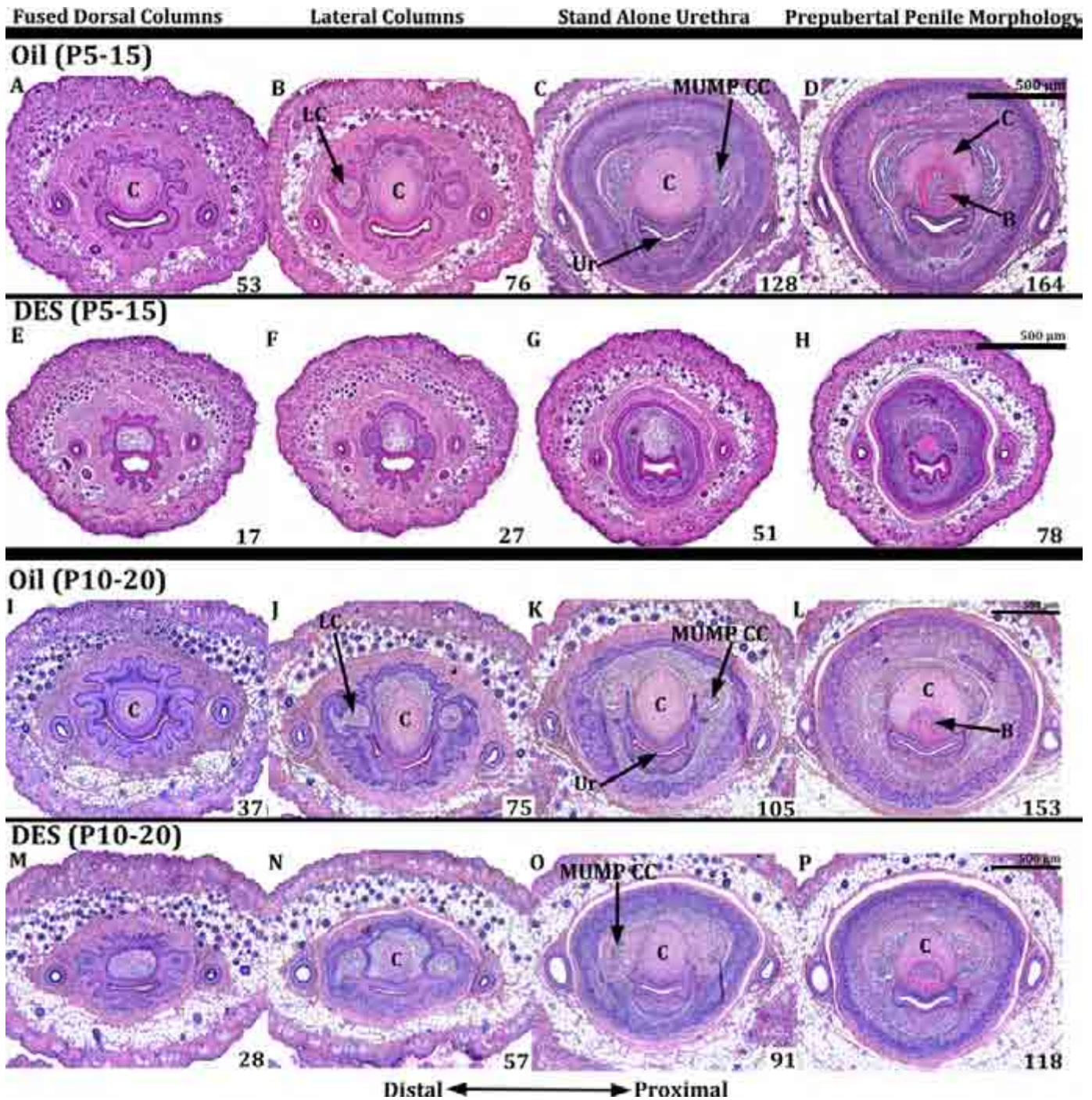


Fig. 8. Transverse serial sections of mouse penises in the oil P5–P15, DES P5–P15, oil P10–P20, DES P10–P20 groups. Sections proceed from distal to more proximal (left to right). Note a reduction in penile diameter (defined by the preputial lamina) in the DES P5–P15 group and the modest reduction in the DES P10–P20 group as compared to oil controls. A DES effect on penile length is also evident. Note that the distance from A to D in the oil P5–P15 groups is 111 sections, whereas this distance is reduced to 61 sections in the DES P5–P15 group. For the oil P10–P20 groups this distance is 116 sections, and in the DES P10–P20 group it is 90 sections. Note also the lack of MUMP cartilage in the DES P0–10 group (E–H), and absence of the MUMP corpus cavernosum (MUMP CC) in the DES P0–10 and DES P5–P15 group (G). The MUMP cartilage and the MUMP corpus cavernosum are present in the DES P10–P20 group (N–P), similar to the oil-treated control (I–L). All images are at the same magnification. LC=lateral mesenchymal column, C=cartilage, B=bone, Ur=urethra.

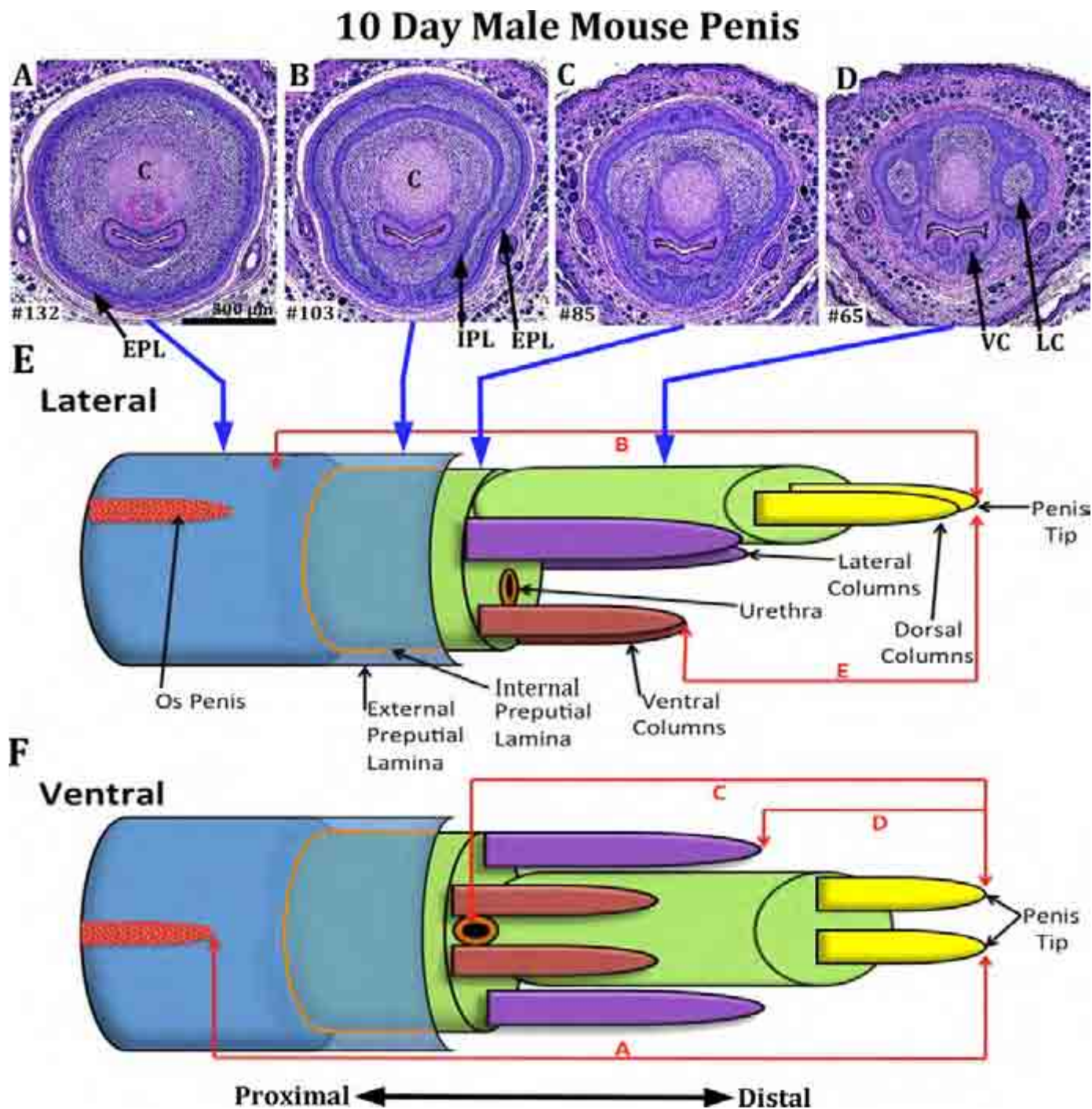


Fig. 9. Schematics (E and F) of a P10 oil-treated penis showing the method of obtaining the measures depicted in Figs. 10 and 11. Morphometric measures are represented by the red lines labeled A, B, C, D and E. Histologic sections (A–D) demonstrate the tissues/structures present at the positions indicated. Note in (A, which represents prepubertal penile morphology) the external preputial lamina surrounds the urethra, tip of the os penis and MUMP cartilage labeled “C”. (B) shows two concentric preputial laminae (internal [IPL] and external [EPL]), the urethra and MUMP cartilage. (C) is the first section containing a “stand alone” urethra. (D) contains the distal aspects of the lateral (LC) and ventral mesenchymal columns (VC). All images are at the same magnification. Abbreviations: C=MUMP cartilage, LC=lateral mesenchymal column, VC=ventral mesenchymal column, IPL= internal preputial laminae, EPL= external preputial laminae.

DES administered during succeeding time frames: E12–E18, E12–P10, P0–P10, P5–P15 and P10–P20. The E12–E18 group was harvested and examined at postnatal day 10, while all of the rest of the specimens were examined 1–2 days after the last injection as described above (Table 1). Developmental montages were constructed with sections arrayed from distal to proximal (Figs. 7 and 8). The first column of Fig. 7 (Fig. 7A–M) labeled “Fused Dorsal Columns” depicts distal sections shortly after the right and left dorsal mesenchymal columns have fused, and thus a MUMP

cartilage and urethra are observed both surrounded by a morphologically complex common epithelium (Fig. 7A–M). Photos in the more proximal second column (labeled “Lateral & Ventral Columns”) were selected to contain both the lateral and ventral mesenchymal columns (Fig. 7B–N). The lateral and ventral mesenchymal columns are the precursors of two types of erectile bodies, namely the MUMP corpora cavernosa and the corpora cavernosa urethrae, respectively (Rodriguez et al., 2011; Rodriguez et al., 2012; Schlomer et al., 2013). The third column labeled “Stand

Alone Urethra" (Fig. 7C–O) is even more proximal and contains the first section containing a "stand-alone" urethra, meaning that the urethral epithelium is not attached to any other epithelial structures. In this third column the penis is defined around its periphery by a preputial lamina but may contain elements of both the internal and external preputial laminae (Fig. 7C–O). The fourth column, the most proximal in the series labeled "Prepubertal Penile Morphology" contains a "stand-alone" urethra, MUMP cartilage, the distal aspect of the os penis, and is defined circumferentially and exclusively by the external preputial lamina (internal preputial lamina is not present this far proximally). Superimposed on each image is a number, which represents the number of 7 μ m sections from the first section having epithelium of the distal tip of the penis to the section in question and thus gives a length measurement of the section relative to the distal aspect of the penis. Examination of these numbers reveals a consistent reduction in overall penile length in all specimens treated with DES and harvested at day 10, namely DES E12–E18, DES P0–P10, and DES E12–P10. For example, the distance in the oil-treated group (Fig. 7A–D) shown in the top row from section 7A to section 7D is 91 sections. In contrast, for the DES E12–E18 group this distance is reduced to 73 sections (Fig. 7E–H), for the DES P0–P10 group the distance is reduced to 51 sections (Fig. 7I–L), and for DES E12–P10 the distance is reduced to 78 sections (Fig. 7M–P). Thus, reduction in overall penile length was greatest in DES P0–P10 group. While the data represented by section number in Figs. 7 and 8 were not analyzed statistically, they give a fair representation of penile size reductions, which are confirmed by statistical analysis of DES-induced alterations in morphology (Figs. 10 and 11), and corroborate previous observations (Mahawong et al., 2014b, 2014a).

For those specimens analyzed at 15 and 20 days postnatal (DES- and oil-treated P5–P15 and P10–P20), a substantial effect on overall penile length was also seen in the DES P5–P15 group (Fig. 8E–H), but less so in the DES P10–P20 group (Fig. 8M–P). For example, the distance from section A to section D in the oil P5–P15 group (Fig. 8A–D) was 111 sections. In contrast, for the DES P5–P15 group the distance between Sections 2E and H was reduced to 61 sections (Fig. 8E–H). For the oil P10–P20 group the overall distance from section 8I to section 8L was 116 (Fig. 8I–L), and for DES E12–P10 the distance from section 8M to section 8P was reduced to 90 sections (Fig. 8M–P).

DES also reduced penile width, although the degree of reduction in penile width varied with the timing of the DES treatment as well as with the proximal-distal position for specimens analyzed at 10 days postpartum (E12–E18, DES P0–P10, DES E12–P10). For example, comparison of oil-treated sections (Fig. 7A–D) with their counterparts in the DES P0–P10 and DES E12–P10 groups revealed a substantial reduction in penile width as defined by the epithelium of the preputial lamina (Compare Fig. 7A–D with sections 7I–P). Reduction in penile width was greatest in the DES E12–P10 group (Fig. 7O and P). This effect was less pronounced in the DES E12–E18 group (Fig. 7G and H). For those specimens analyzed at 15 and 20 days postnatal (DES- and oil-treated P5–P15 and P10–P20), reduction in penile width was modest in the DES P5–P15 group and negligible in the DES P10–P20 group (Fig. 8). Taken together, DES treatment during penile development reduces both penile length and width, thus corroborating previous studies (Mahawong et al., 2014b, 2014a).

3.1. Morphometric analysis

Measures were taken of various penile elements in the DES- and oil-treated groups at 10, 15 and 20 days postnatal. For this analysis the distal starting point for all measurements was the first distal section containing penile stroma, namely the bilateral dorsal mesenchymal columns. Fig. 9 provides drawings indicating how

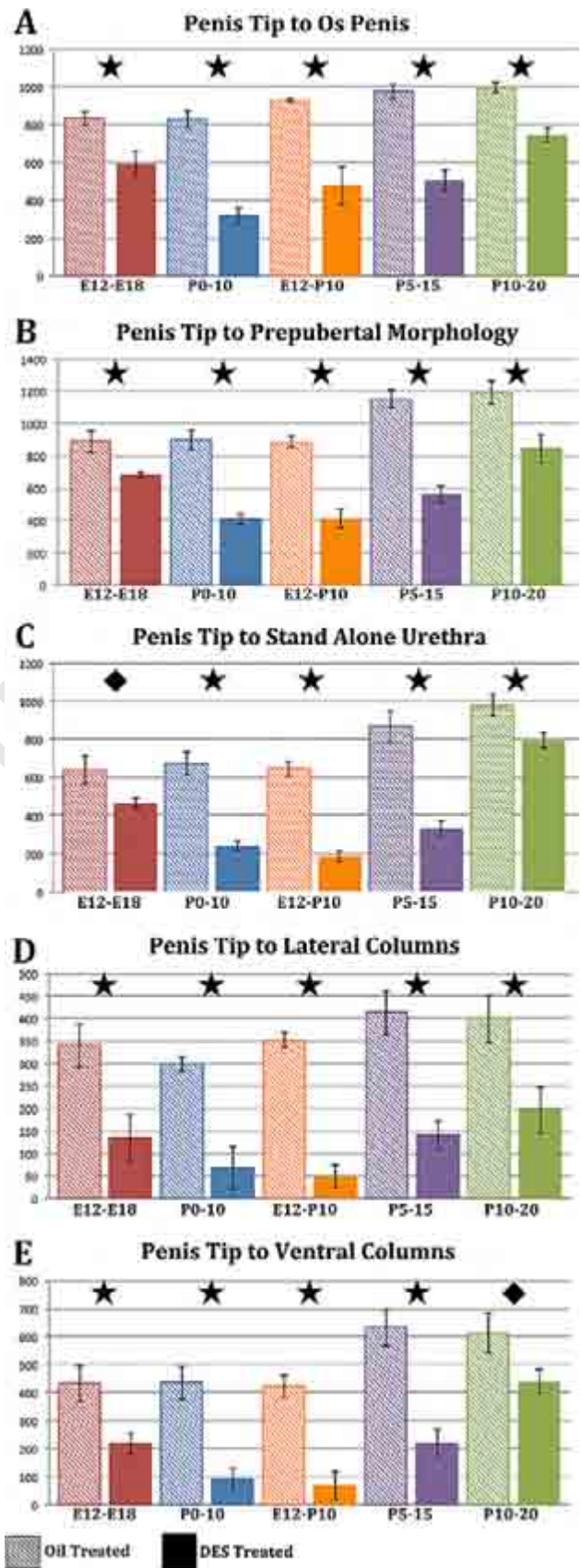


Fig. 10. Morphometric measures of distal tip of penis to os penis (A), distal tip of penis definitive prepubertal morphology (B) as defined in Fig. 11A, distal tip of penis to "stand alone" urethra (C), distal tip of penis to distal tip of the lateral columns (D), and distal tip of penis to distal tip of the ventral columns (E). All measurements are in micrometers. For statistical significance, a "p" value of ≤ 0.05 is represented by +, " $p \leq 0.001$ " by *, and " $p \leq 0.0001$ " by *.

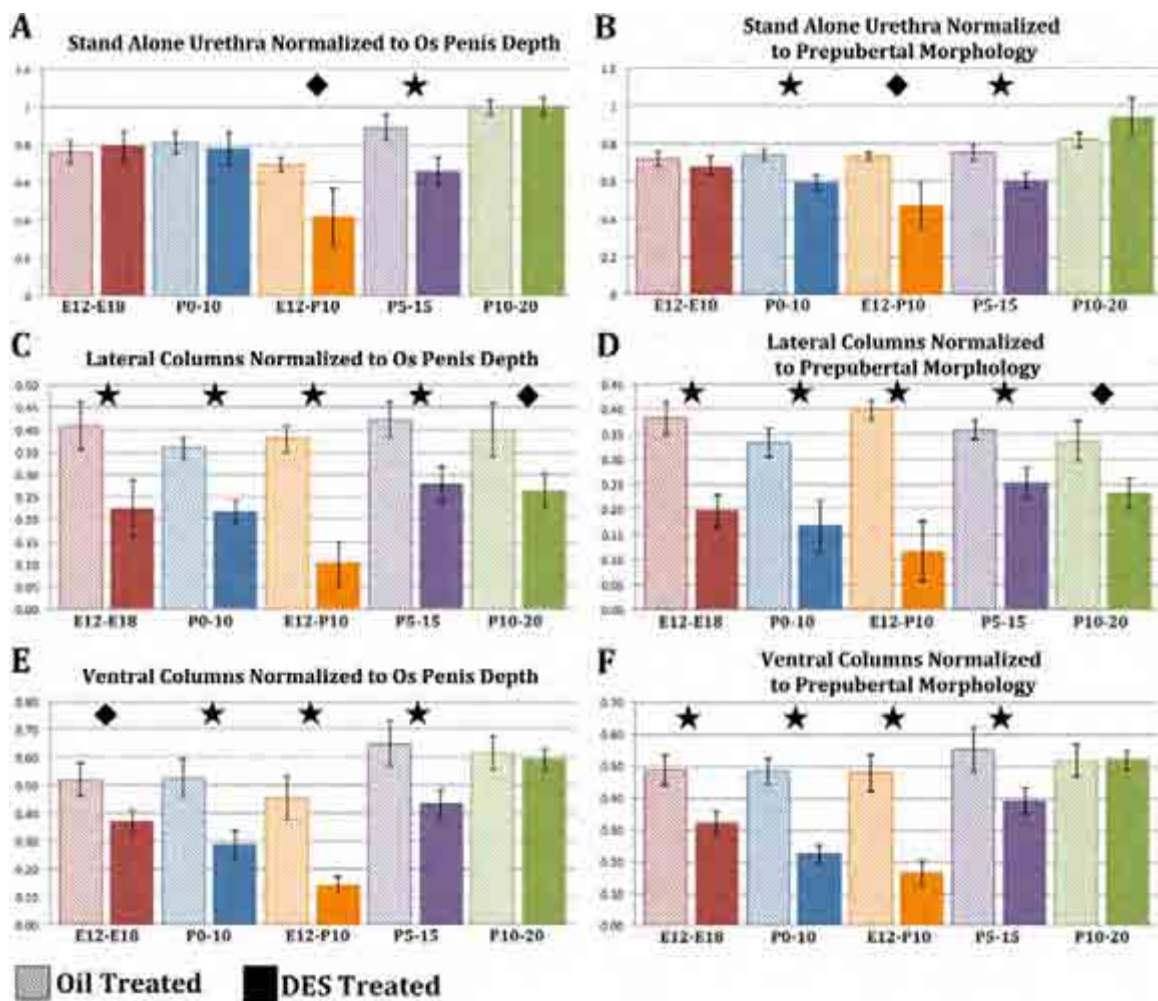


Fig. 11. Morphometric measures normalized to surrogates of penile length (distal penile tip to os penis [os penis depth, A, C, E] or to prepubertal morphology [B, D, F]). The morphometric measures normalized to os penis depth are: distal tip of penis to “stand alone” urethra (A), distal tip of penis to distal tip of the lateral columns (C), distal tip of penis to distal tip of the ventral columns (E). The morphometric measures normalized to prepubertal morphology are illustrated in (B, D, and F). All measurements are in micrometers. For statistical significance, a “p” value of ≤ 0.05 is represented by +, “p” ≤ 0.001 by ◆, and “p” ≤ 0.0001 by ★□□□□□□□□□□ oil-treated control.

each measurement was derived and also gives the histology of a P10 oil-treated specimen indicating the tissues/structures present at the positions indicated. Fig. 9A contains a stand-alone urethra, MUMP cartilage, the tip of the os penis and the external preputial lamina and thus represents “prepubertal penile morphology” (also illustrated in Fig. 7D). External (EPL) and internal preputial laminae (IPL), MUMP cartilage and the urethra are seen in Fig. 9B. The first section containing the “stand alone” urethra is seen in Fig. 9C. Lateral (LC) and ventral columns (VC) are seen in Fig. 9D. Since a perfectly vertical orientation of a specimen in the paraffin block was rarely achieved, the right and left dorsal, lateral, and ventral mesenchymal columns typically were found in different, but closely situated sections. Consequently, the average was taken between the start of the right and left dorsal, lateral, and ventral columns to account for variation in orientation of the specimens. Accordingly, the position of the “stand-alone” urethra (Fig. 9C) was determined by counting the number of 7 μ m sections (and thus computing the distance) from the average distal tip of the dorsal mesenchymal columns to the point where the urethral epithelium was not in contact with any other epithelia, and thus the urethra was completely circumferentially surrounded by penile stromal tissue (“stand-alone” urethra) (also illustrated in Fig. 7C, G, K, O). Other measures, also determined from the distal tip of the dorsal mesenchymal columns, are indicated in Figs. 10 and 11 and described below.

3.1.1. Prenatal DES (E12–E18) analyzed on day P10

Given that overall penile length was consistently reduced in all DES-treated specimens (Figs. 7 and 8), individual distances were measured from the distal tip of the penis (distal tip of the dorsal mesenchymal columns) as illustrated in Fig. 9. All measurements (Fig. 10) were significantly reduced in DES-treated mice versus oil-treated controls. These included distal tip of penis to distal tip of os penis (Fig. 10A), distal tip of penis to “Prepubertal penile morphology” (Figs. 7D, 10B), distal tip of penis to the first section containing a “stand alone” urethra (Fig. 10C), distal tip of penis to distal tip of the lateral columns (Fig. 10D), and distal tip of penis to distal tip of the ventral columns (Fig. 10E).

3.1.2. Pre + Postnatal DES E12–P10 analyzed on day P10

As above, all penile morphological measures were significantly reduced in DES P0–P10 mice relative to oil-treated controls (Fig. 10). This included measurements of distance from the distal penile tip (distal tip of dorsal mesenchymal columns) to distal tips of the lateral mesenchymal columns and ventral mesenchymal columns, distal penile tip to the “stand alone” urethra, distal penile tip to distal tip of the os penis, and distal tip of penis to “mature penile morphology” (Fig. 10).

3.1.3. Postnatal DES (P0–P10 and P5–P15) analyzed on day P10 and day P15

All penile morphological measures were significantly reduced

in DES P0–P10 and DES P5–P15 mice relative to oil-treated controls (Fig. 10) using the strategy described above.

3.1.4. Postnatal DES (P10–P20) analyzed on day 20

DES treatment from P10 to P20 also reduced all of the morphometric measures (Fig. 10). However, it should be noted in both the P5–P15 and the P10–P20 groups that lengths observed in the oil-treated groups were trending higher as is appropriate for their older age.

In summary, the general pattern seen for all measures demonstrated that the greatest reductions for each distance measure were seen in the DES P0–P10, E12–P10 and P5–P15 groups, with more modest effects of DES seen in the E12–E18 and the P10–P20 groups, thus defining a distinct “programming window” for the adverse effects of DES.

3.2. Normalization of morphometric data

Given the reduction in overall penile length as described in Figs. 7 and 8, it is not surprising that individual penile measures were accordingly reduced (distal tip of penis to distal tip of the lateral column, distal tip of penis to distal tip of the ventral columns, distal tip of penis to start of the bone, distal tip of penis to “stand alone” urethra, and distal tip of penis prepubertal penile morphology) (Fig. 10). However, to account for the impact of overall reduction in penile length, each of the above measures was normalized to surrogates of overall penile length, namely normalization to (a) distal penile tip to distal tip of the os penis (os penis depth) or (b) distal penile tip to the first section containing “prepubertal penile morphology” (Fig. 11). This approach further validated the “window of susceptibility” to adverse effects of DES.

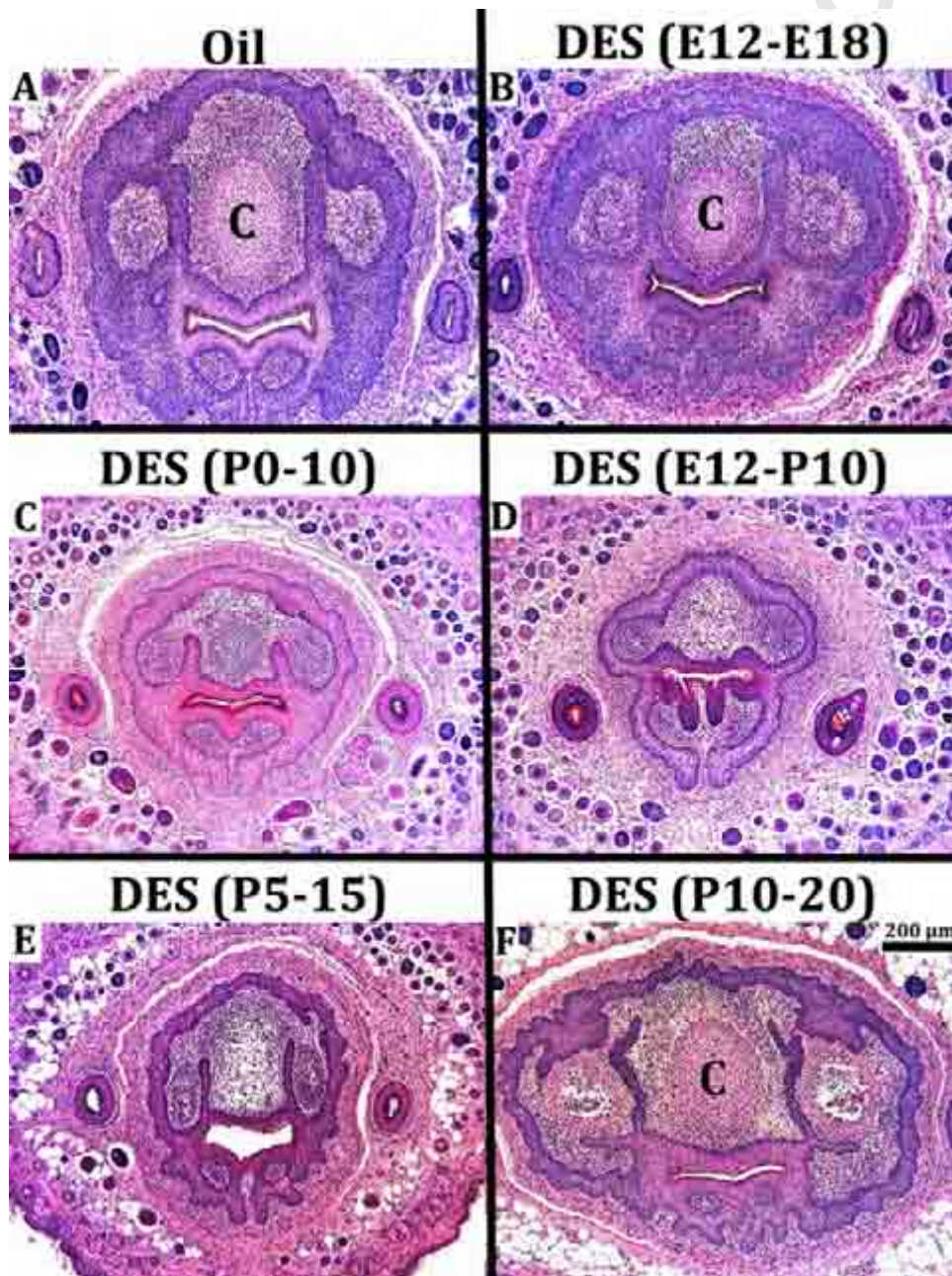


Fig. 12. Transverse H&E sections illustrating DES-induced inhibition of MUMP cartilage differentiation in penile specimens harvested at day 10 postnatal (A–D) or at 15 or 20 days postnatal (E and F, respectively). The MUMP cartilage is seen in the oil-treated control (A), and in the DES E12–E18 and the DES P10–P20 specimens (B and F). Impaired MUMP cartilage differentiation is seen in the DES P0–P10, DES E12–P10, and DES P5–P15 groups (C, D and E). All images are at the same magnification. C=cartilage.

One consequence of this type of normalization is that the reduction in overall penile length coupled with proportional reduction in individual measures resulted in an absence of significant change for some individual measures relative to the oil-treated controls (Fig. 11A and B). However, in the case of the measure of distal penile tip to “stand alone urethra”, significant reductions were observed in the DES E12–P10 and the DES P5–P15 groups when normalized to either os penis depth or prepubertal penile morphology (Fig. 11A and B). Likewise, measures of from the distal penile tip to the lateral or ventral columns, when normalized to either os penis depth or prepubertal penile morphology remained significantly shorter in almost all treatment groups (Fig. 11C, D, E and F). This means that these measures were reduced to a greater extent than “overall penile length”. These data further highlight a

“window of susceptibility” to adverse effects of DES, which is centered from days P0 to P15.

3.3. Effect of DES on differentiation of the MUMP cartilage and erectile bodies

The MUMP cartilage (Fig. 12A) develops secondary to fusion of the dorsal mesenchymal columns (Rodriguez et al., 2011; Schlomer et al., 2013). The significance of the MUMP and its cartilage is that it forms part of the urethral meatus whose morphology is malformed in hypospadias. At day 5 the mesenchymal condensation representing the MUMP cartilage is beginning to differentiate (not illustrated), and at day 10 postnatal MUMP cartilage differentiation is advanced (Figs. 7A–D and 12A). In male CD1 mice treated

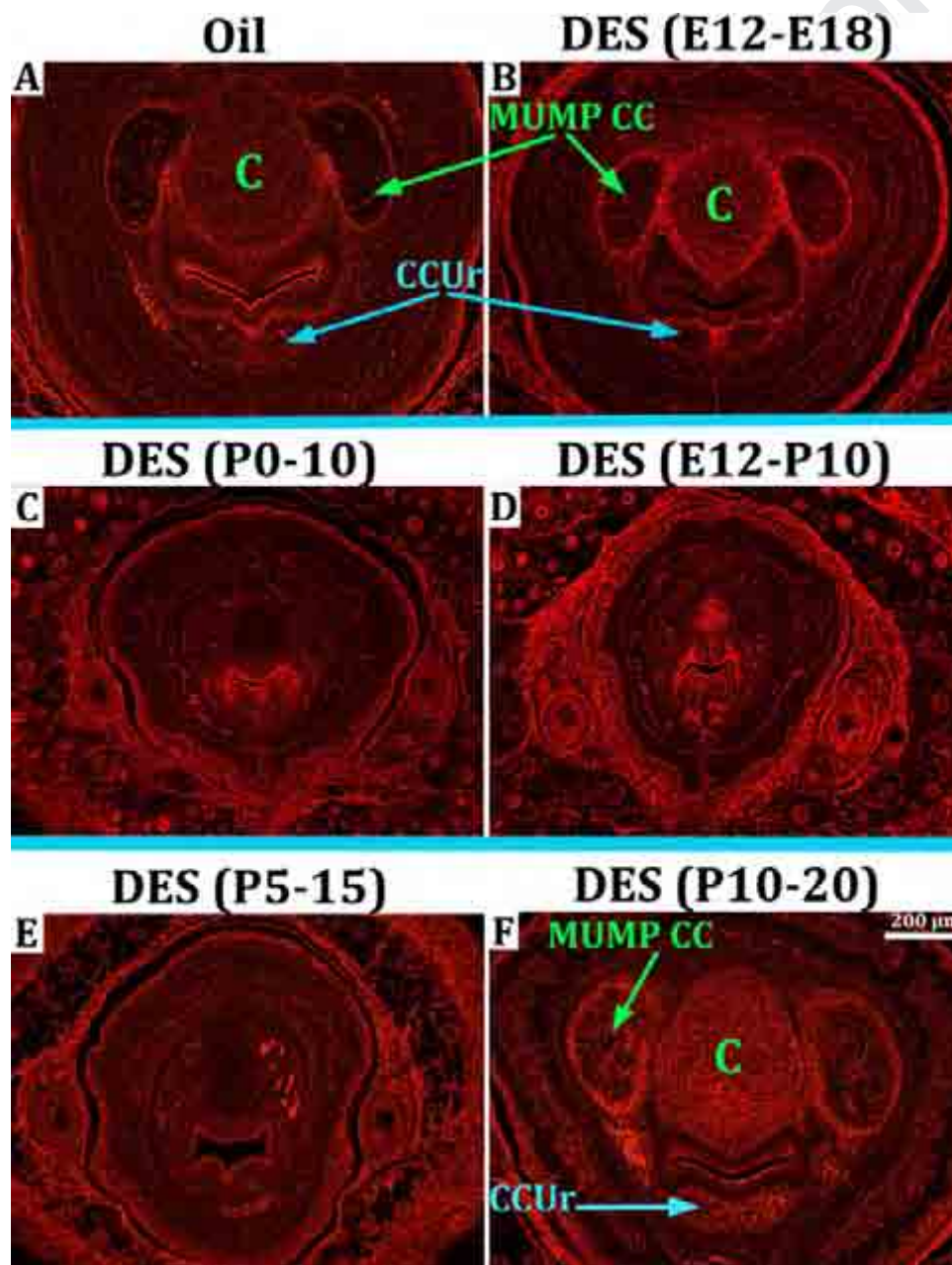


Fig. 13. Epifluorescence of transverse H&E sections illuminated with Cy3 HYQ filter combination illustrating DES-induced inhibition of erectile body development (the MUMP corpora cavernosa [MUMP CC] and the corpora cavernosa urethrae [CCUr]) in penile specimens harvested at day 10 postnatal (A–D) or at 15 or 20 days postnatal (E and F, respectively). The MUMP corpora cavernosa (MUMP CC) and the corpora cavernosa urethrae (CCUr) are seen in the oil-treated control (A), and in the DES E12–E18 (B) and the DES P10–P20 specimens (F). Impaired development of the MUMP corpora cavernosa and the corpora cavernosa urethrae is seen in the DES P0–P10 group (C) and DES E12–P10 group (D), and the DES P5–P15 group (E). MUMP cartilage is denoted by the label “C”. All images are at the same magnification.

prenatally (E12–E18) with DES, the MUMP cartilage was well differentiated when examined at 10 days postnatal (Fig. 12B). However, in this group (DES E12–E18), DES treatment terminated well before differentiation of the MUMP cartilage and thus was without effect when observed at day 10 postnatal. In contrast, the MUMP cartilage was undifferentiated and represented by a mesenchymal condensation in the DES P0–P10 group when examined at 10 days postnatal (Fig. 12C). Impairment of MUMP cartilage differentiation was particularly profound in mice treated with DES pre- and postnatally (DES E12–P10) when examined on day 10, as most specimens lacked the mesenchymal condensation (Fig. 12D). Mice treated with DES from days P5–P15 and examined on day 15 also exhibited impaired MUMP cartilage differentiation similar to the DES P0–P10 (Fig. 12E). In contrast, mice treated with DES from P10 to P20 (after initiation of MUMP cartilage differentiation) exhibited a normal MUMP cartilage on day 20 (Fig. 12F).

The effect of DES was examined on two erectile bodies, namely the MUMP corpora cavernosa and the corpora cavernosa urethrae, the homolog of the human corpus spongiosum. The MUMP corpora cavernosa (MUMP CC) are bilateral erectile bodies that develop just lateral to the MUMP cartilage (Fig. 13A) (Rodriguez et al., 2011). The corpora cavernosa urethrae are an erectile bodies that develop ventral to the urethra (Rodriguez et al., 2011) (Fig. 13A). In oil-treated mice at postnatal day 10 the MUMP corpora cavernosa and the corpora cavernosa urethrae are well formed and clearly demarcated by circumferential capsules of smooth muscle (Fig. 13A). In mice treated with DES from E12 to E18, the MUMP CC and the corpora cavernosa urethrae were present but reduced somewhat in size when examined at day P10 (Fig. 13B). In mice treated with DES from P0 to P10, the MUMP corpora cavernosa and the corpora cavernosa urethrae were absent when examined at day P10 (Fig. 13C). Mice treated with DES from E12 to P10 also exhibited profound impairment in development of the MUMP corpora cavernosa and the corpora cavernosa urethrae (Fig. 13D). The MUMP corpora cavernosa and the corpora cavernosa urethrae were also absent in mice treated with DES from P5 to P15 when examined at day P15 (Fig. 13E). In the DES P10–P20 group, the MUMP corpora cavernosa and the corpora cavernosa urethrae were well developed and of similar size as that of oil-treated controls when examined at P20 (Fig. 13F and Table 2).

Effects of DES on the MUMP cartilage, MUMP corpora cavernosa and the corpora cavernosa urethrae led to either temporary or permanent adult malformations depending on the timing of DES treatment. This was assessed by treating mice with DES during the periods described above and then assessing results at 60-days postpartum. In this experiment impaired MUMP cartilage differentiation observed at day P10 in the DES P0–P10 and E12–P10 groups (Fig. 14I and J) remained defective when DES P0–P10 and E12–P10 mice were aged to 60 days postnatal (Fig. 14C and D),

indicating that impaired MUMP cartilage differentiation seen developmentally endured into adulthood as presumably an irreversible DES effect. MUMP cartilage differentiation was also impaired in DES P5–P15 mice when observed at day P15 (Fig. 14K), but fully recovered by day P60 (Fig. 14E). In the oil-treated control group, DES E12–P10 and DES P10–P20 groups, the MUMP cartilage was well differentiated at P10, P20 as well as at P60. Thus, the effect of DES on MUMP differentiation exhibited a “window of susceptibility” to the adverse effects of DES from P0 to P15. More important, the adverse effects of DES on MUMP cartilage differentiation were permanent and presumably irreversible in the DES P0–P10 and DES E12–P10 groups, but reversible in the DES P5–P15 group,

DES had a similar effect on development of the MUMP corpora cavernosa. The MUMP corpora cavernosa were absent or ill defined in DES P0–P10, DES E12–P10 and DES P5–P15 groups when assessed at days P10 or P15 (Fig. 14I–K). The MUMP corpora cavernosa remained indistinct or ill defined in DES P0–P10 and DES E12–P10 mice when aged to day P60 (Fig. 14C and D), but fully recovered in the DES P5–P15 group (Fig. 14E). For all other groups (Oil control [Fig. 14A and G], DES E12–E18 [Fig. 13B and H], and DES P10–P20 [Fig. 14F and L]), the MUMP corpora cavernosa were present developmentally at day P10 or P20 and also present at day P60. Thus, the pattern of DES effects and reversibility for the MUMP corpora cavernosa were similar to that observed for the MUMP cartilage.

4. Discussion

Development of the male reproductive tract is sensitive to steroidal sex hormones. Masculine development of the reproductive tract, including the external genitalia, is elicited by fetal testicular androgens (Wilson et al., 1981). However, for each structure (Wolffian duct, urogenital sinus and external genitalia) there exists a masculinizing programming window during which the presence of androgens is required and during which anti-androgens can inhibit masculine development (Welsh et al., 2007, 2008; Macleod et al., 2010; Welsh et al., 2010). Based upon studies involving the administration to pregnant rats of the anti-androgen, flutamide, the critical window for masculine development of the Wolffian duct (the precursor of the epididymis, vas deferens and seminal vesicle) is between E15.5 and E17.5. Induction of hypospadias with flutamide in male rats has a timing window of E15.5–E19.5, meaning that normal masculinization of the external genitalia requires androgen action from E15.5 to E19.5 (Welsh et al., 2008). In the current paper we explored the programming window for DES-induced abnormal development of the male external genitalia.

Hypospadias is fundamentally an alteration in the position of the urethral meatus associated with abnormal patterning or absence of elements (external features as well as internal structures) within the penis. For example, in human midshaft hypospadias, the abnormal position of the midshaft urethral meatus is associated with absence or defects in the following structures: (a) ventral penile skin, (b) ventral urethral epithelium, (c) corpus spongiosum (Cunha et al., 2015b) (Fig. 15). Mice treated with DES from E12–E18 and assessed at day 60 postnatal exhibited (a) an altered patterning of the elements constituting the urethral meatus, (b) altered patterning of the positions of the urethral flaps and the distal tip of the os penis relative to the open ventral cleft in the MUMP ridge and (c) reduction in MUMP length, individual features that are elements indicative of hypospadias (Mahawong et al., 2014b). In contrast, mice treated with DES from P0 to P10 and assessed at day 60 postnatal exhibited even more profound penile defects: (a) severe truncation of the prepuce and glans

Table 2
Effects^a of DES on the MUMP cartilage, erectile bodies and penile size.

Harvest age	Treatment periods	Comparison to oil-treated		
		MUMP cartilage	Erectile bodies	Penis size
10 day	Prenatal DES (E12–E18)	Near normal	Near normal	Smaller
10 day	Postnatal DES (P0–P10)	Absent	Absent	Much smaller
10 day	Pre- and Postnatal DES (E12–P10)	Absent	Absent	Much smaller
15 day	Postnatal DES (P5–P15)	Absent	Absent	Smaller
20 day	Postnatal DES (P10–P20)	Near normal	Near normal	Near normal

^a Measurements were taken at day 10, 15 or 20 as described above.

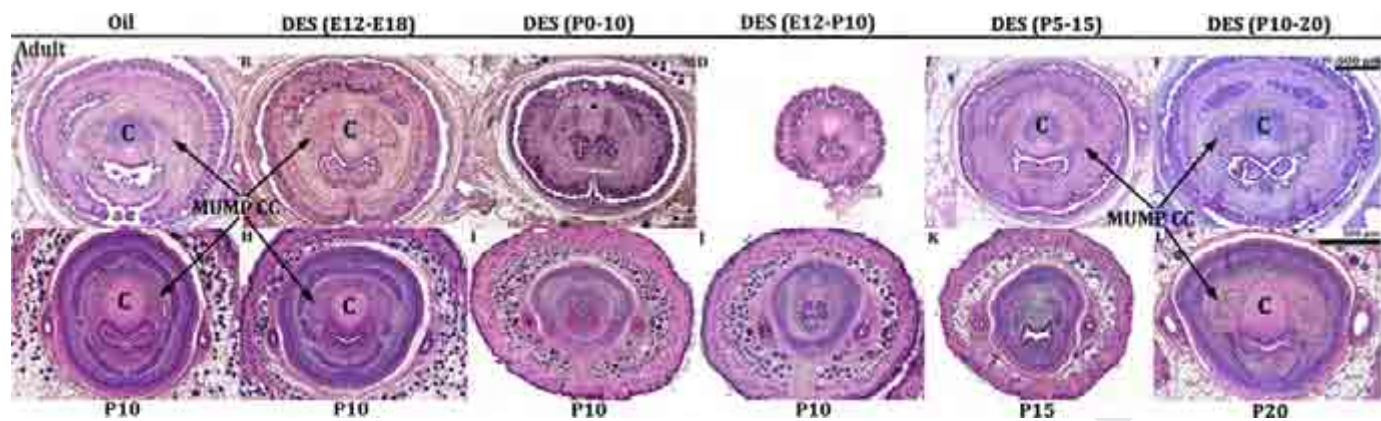


Fig. 14. Transverse H&E sections of oil- and DES-treated penises as indicated harvested at 60-days postnatal (top row, A–F) or at P10 (G–J), P15 (K) or P20 (L) (bottom row) at the level of the MUMP cartilage (denoted by “C”) and MUMP corpora cavernosa (MUMP CC). Note the inhibition of MUMP cartilage and the MUMP corpora cavernosa at day 10 in the DES P0–P10 (I) and DES E12–P10 (J) groups results in an absence of MUMP cartilage differentiation at day 60 postpartum (C and D). In contrast, inhibition of MUMP cartilage at day 15 in the DES P5–P15 group (K) leads to MUMP cartilage recovery at 60 days postpartum (E). MUMP cartilage and the MUMP corpora cavernosa were normal at both day 10 and at day 60 in the oil-treated group (A and G) and in the DES E12–E18 (B and H) and DES P10–P20 groups (F and L). All images are at the same magnification.

penis, (b) an abnormal urethral meatus, (c) ventral tethering of the penis (a defect in ventral penile skin), (d) reduced os penis length and glans width, (e) impaired differentiation of the MUMP cartilage, (f) absence of urethral flaps, and (g) impaired differentiation of erectile bodies (Mahawong et al., 2014a). These data indicate that the types of malformations indicative of hypospadias vary depending on the timing of DES exposure. In mice treated with DES on days E12–E18 and on days P0–P10, penile malformations enduring into adulthood (P60) meet the general definition of hypospadias in so far as the shape and patterning of the urethral meatus is highly abnormal, and patterning of a variety of internal structures is substantially altered relative to the ventral urethral groove (Mahawong et al., 2014b; Cunha et al., 2015b). It is important to note the homology between the human corpus spongiosum and the mouse corpora cavernosa urethrae (both are erectile bodies intimately associated with the urethra). Thus, the DES-induced malformation in the mouse corpora cavernosa urethrae is a direct counterpart to the defective corpus spongiosum seen in human hypospadias (Cunha et al., 2015b). While the malformations seen in prenatally and neonatally DES-treated mice meet the general definition of hypospadias, they are vastly different from the dramatic midshaft or perineal urethral defects seen in human hypospadias (Cunha et al., 2015b), suggesting important differences in the morphogenetic mechanism of penile development in mice versus humans.

Our previous studies of the effect of DES on the developing mouse penis utilized two treatment protocols, prenatal only (E12–E18) and postnatal only (P0–P10), with specimens examined at 60 days postpartum to assess malformations enduring into adulthood (Mahawong et al., 2014b, 2014a). In the present paper the periods of DES treatment were extended to encompass a wider age range and thus have demonstrated a definite “window of susceptibility” to the adverse effects of DES for many parameters within the developing mouse penis. Our earlier studies demonstrated that the types of malformations observed at 60 days postnatal were different based upon whether the DES treatment was prenatal (E12–E18) or postnatal (P0–P10) (Mahawong et al., 2014b, 2014a). DES-induced reduction in penile length and width were confirmed in the present paper and are presumably mediated via signaling through estrogen receptors alpha and/or beta (ER α and ER β), which have been previously detected in all of the structures affected by DES (dorsal, ventral and lateral mesenchymal columns, MUMP cartilage, urethra, preputial lamina and developing erectile bodies) (Rodriguez et al., 2012; Blaschko et al., 2013). Attenuation of penile length and width in response to DES may be due to

inhibition of cell proliferation, although this was not examined in the present study, and effects on apoptosis also need to be considered.

Additional treatment protocols were used in the present investigation to define a “window of susceptibility” to the adverse effects of DES on the developing mouse penis. Based upon several (but not all) DES-affected parameters, the “window of susceptibility” to the adverse effects of DES for many elements within the penis is centered in the period from P0 to P15 during which DES elicited overall reduction in penile length and width, impaired MUMP cartilage differentiation, impaired erectile body development, as well as affected a range of morphometric parameters reflective of abnormal patterning of penile elements (measures of distal penile tip to distal tip of the os penis, distal penile tip to beginning of the external preputial lamina, distal penile tip to “stand-alone” urethra, and distal penile tip to the distal tips of the lateral and ventral mesenchymal columns). For mice treated before or after this “window of susceptibility” (DES E12–E18 and DES P10–P20), the adverse effects of DES were substantially attenuated or completely absent, indicative of treatment outside of the optimal DES programming window, presumably based upon the fact that many of the individual elements within the penis are already in place and well differentiated prior to initiation of DES treatment at day 10 or that the DES treatment period occurred substantially before a particular developmental process. Fig. 10, a detailed morphometric analysis, demonstrates that DES-induced morphometric alterations are most profound in the P0–P10, E12–P10 and P5–P15 groups, with more modest effects seen in the E12–E18 and P10–P20 groups. Thus, DES exposure encompassing postnatal periods had the greatest effects even though effects of DES were also seen in the prenatal only DES group. Figs. 7 and 8 illustrating histology at defined proximal-distal locations are also consistent with enhanced DES susceptibility in the neonatal period (P0–P15). The apparent modest effects of DES seen in the E12–E18 group deserve comment and may be due to the ~11-day recovery period associated with this treatment group as injections of DES on days E12–E18 day were followed by ~11 days of recovery before harvest at day P10. For all other treatment groups the specimens were harvested within 1–2 days of the last DES injection.

Given that DES elicits an overall reduction in penile length, the concomitant reductions in distances between the distal penile tip and several other penile elements (measures of distal penile tip to distal tip of the os penis, distal penile tip to beginning of the external preputial lamina, distal penile tip to “stand-alone” urethra, and distal penile tip to the distal tips of the lateral and ventral

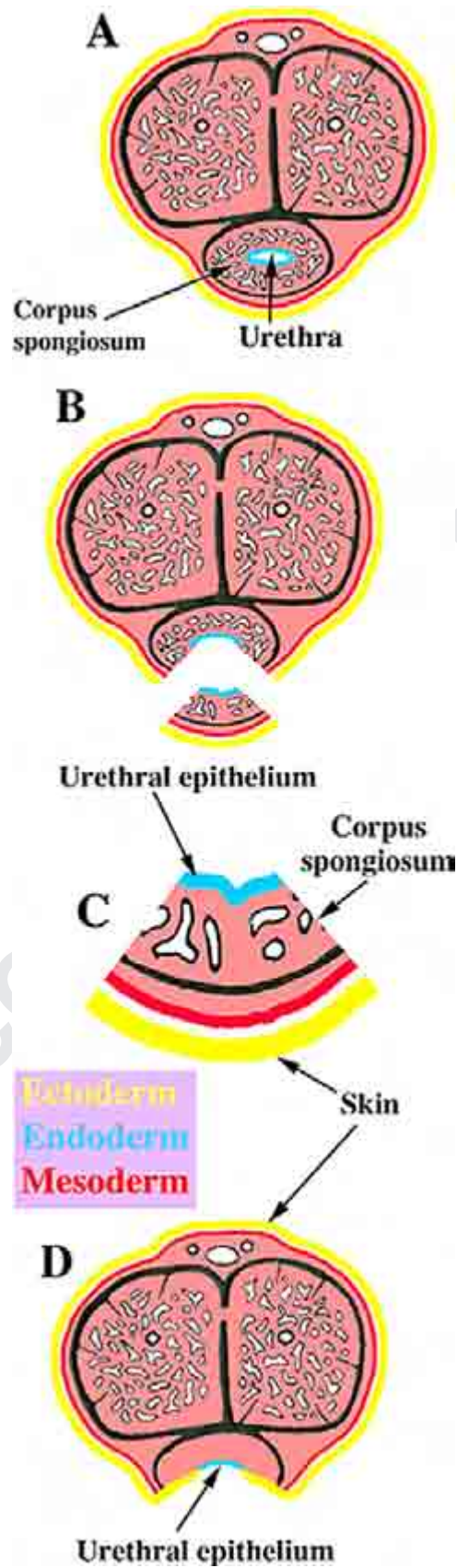


Fig. 15. Drawings of transverse sections through the normal human penis (A) as well as through human midshaft hypospadias illustrating the penile elements defective/absent in human hypospadias (B–D). In the region just distal to the midshaft urethral meatus, the elements missing from the penis are the ventral urethral epithelium, the corpus spongiosum and the ventral penile skin (C). Urethral epithelium (endoderm) is in blue, skin is in yellow (ectoderm), all other internal structures are flesh colored (mesoderm). Adapted from Mahawong et al. (2014b) with permission. (For interpretation of the references to color in this figure legend, the reader is referred to the web version of this article.)

mesenchymal columns) were expected especially for those specimens treated with DES during the “window of susceptibility” (Fig. 10). However, when DES-induced alterations in morphometric features were normalized to surrogates of penile length (distal penile tip to distal tip of os penis or distal penile tip to prepubertal morphology as defined in Fig. 7D), statistical significance of many of the measures disappeared, meaning that reduction in overall penile length was proportional with length reductions of individual penile elements. However, measures involving the position of the “stand alone urethra”, lateral and ventral mesenchymal columns exhibited statistically significant reductions relative to oil-treated controls when normalized to surrogates of penile length, again in the P0–P15 treatment period (Fig. 11). These observations further reinforce a “window of susceptibility” to adverse effects of DES during the neonatal period and also indicate that differential response of individual morphometric measures will necessarily lead to alterations in morphologic patterning of penile elements in so far as individual morphometric measures may exhibit enhanced susceptibility to DES relative to overall generalized reduction in penile length.

An important lesson from our past studies is that it is critical to assess penile malformations in adulthood since several types of penile malformations seen at the end of gestation or in the neonatal period may revert to normality when prenatally or neonatally estrogen-treated mice are allowed to age to adulthood (Cunha et al., 2015b). For example, observations of an open urethral groove on the distal aspect of the embryonic mouse genital tubercle have been designated as “hypospadias” in several publications. In an earlier study of ours pregnant mice were treated with 17 α -ethinyl estradiol or DES from days 12–17 of gestation and analyzed at 18 days of gestation. Such prenatally estrogen-treated mice exhibited an extensive open “urethral” groove in the embryonic genital tubercle (reported as hypospadias) with an incidence of 40–57% ($N=134$) (Kim et al., 2004). The tacit (but unproven) assumption is that embryonic genital tubercle malformations are irreversible and progress to enduring adult penile malformations, even though in most cases embryonic genital tubercle defects were not allowed to progress to their definitive adult penile phenotype(s). In a recent study replicating the Kim et al. protocol, 57 mice were treated in utero with DES from P12 to P17, and then aged to P60. Expected midshaft penile urethral hypospadias was not observed in adulthood ($N=0/57$) (Mahawong et al., 2014b). Similarly, Iguchi et al. reported “hypospadias” at the end of gestation in mice treated with a 5 α -reductase inhibitor, but hypospadias was not found when assessed at 90 days postnatal (Iguchi et al., 1991). We can now add the MUMP cartilage and erectile bodies to the list of examples of “embryonic/neonatal malformations” that revert to normality when perinatally DES-treated mice are allowed to age to adulthood, suggesting that some developmental effects of perinatal DES are mere retardations in development which revert to normality given sufficient time. Whether an estrogen-induced anomaly observed in the perinatal period persists into adulthood or reverts to normality is a function of the timing of estrogen treatment. For the DES E12–P10 and the DES P0–10 groups impaired MUMP cartilage and erectile body differentiation observed in the neonatal period persisted into adulthood and thus appear to be irreversible. In contrast, similar anomalies seen developmentally in the DES P5–P15 group reverted to normality at 60 days postpartum.

In addition to effects on various length/width parameters, DES also affected differentiation of the MUMP cartilage known to express ER α and ER β (Rodriguez et al., 2012; Blaschko et al., 2013). The MUMP and its cartilage develop from a mesenchymal condensation secondary to fusion of the right and left dorsal mesenchymal columns (Schlomer et al., 2013), which occurs in the early neonatal period. In the case of mice treated from E12 to E18,

MUMP cartilage differentiation assessed at day 10 was fairly normal. This result may be due to the fact that the period of DES treatment terminated before normal initiation of MUMP cartilage differentiation, and that any effect of prenatal DES treatment on cartilage differentiation may have recovered during the \sim 11 days after cessation of DES treatment. In contrast, DES treatment during the P0–P15 time frame (E12–P10, P0–P10, P5–P15) elicited profound inhibition of MUMP cartilage differentiation in specimens analyzed shortly after the last DES injection. DES treatment from P10 to P20 had minimal effects on MUMP cartilage differentiation when assessed at P20. Taken together, these data corroborate a “window of susceptibility” to the adverse effects of DES in the period P0–P15 as suggested above. Likewise, development of erectile bodies (the MUMP corpora cavernosa and the corpora cavernosa urethrae) exhibit an almost identical time course of DES-induced impairment. In the DES P5–P15 group the impaired differentiation of the MUMP cartilage and MUMP corpora cavernosa seen at day P15 was merely a retardation of development since both parameters reverted to normal when the mice of this treatment group were allowed to age to 60 days (Fig. 14E). Thus, possible reversion of a developmental abnormality to normality in adulthood is a function of the timing of DES treatment, with the most profound effects and thus the absence of reversion to normality being seen in the P0–P10 and E12–P1 DES groups. Accordingly, while recovery to normality is possible for certain penile features, others are not and result in enduring malformations into adulthood depending on the timing of DES exposure.

Estrogen-induced mouse hypospadias involves malformation of the urethral meatus and abnormal patterning of distal elements of the penile urethra, but not midshaft, scrotal or perineal hypospadias as is the case for human and rat (Clark et al., 1990; Bowman et al., 2003; Cunha et al., 2015b). At this date, this conclusion is based upon analysis of 138 mice in 3 papers, the current paper and 2 others (Mahawong et al., 2014b, 2014a). The apparent absence of estrogen-induced midshaft hypospadias may be related to the fact that development of the mouse penile urethra occurs in two phases. Prenatally, most of the penile urethra develops within the embryonic genital tubercle via canalization of the urethral plate to form most of the penile urethra, and especially the midshaft region of the urethra (Hynes and Fraher, 2004a, 2004b; Seifert et al., 2008). Postnatally, the urethral meatus forms via fusion of elements that constitute the urethral meatus, a process inferred from direct observations of a prominent mid-ventral penile cleft, as well as adult raphes, circumferential clefts and abnormalities of the urethral meatus elicited by estrogens (Baskin et al., 2001b; Yucel et al., 2003; Blaschko et al., 2013; Mahawong et al., 2014b, 2014a). None (0/138) of the perinatally DES-treated mice examined at 60 days postnatal exhibited midshaft hypospadias even though other malformations were observed in some treatment groups as described above. These data based upon analysis of 138 DES-treated specimens in 3 papers raise the possibility that midshaft hypospadias may not be possible in mice, even though such malformations have been reported in rats treated with “androgen blockers” (flutamide, finasteride, vinclozolin, procymidone, linuron, as well as a variety of phthalates) (Gray et al., 1994; Ostby et al., 1999; Wolf et al., 1999; Bowman et al., 2003; Foster and Harris, 2005; Rider et al., 2008; Rider et al., 2009).

Day 10 postnatal was selected as a common time point for analysis of most of the specimens because it represents a critical time point in the genesis of penile malformations. Based upon observations in this paper, we can now recognize those developmental perturbations at day 10 that will lead to enduring adult penile malformations. Some of the 10-day DES-induced malformations are morphologic such as reduction in penile length and width and perturbation of erectile body development, which are best observed in serial histologic sections as illustrated in

Figs. 7 and 8. Impaired MUMP cartilage differentiation is a notable malformation seen at day 10 in the DES E12–P10 and DES P1–P10 treatment groups that lead to enduring adult malformation of not only the MUMP cartilage, but also to an abnormal urethral meatus and other penile defects (Mahawong et al., 2014a). Thus, estrogen-induced impaired MUMP cartilage differentiation can be used as an indicator of penile malformations leading to irreversible malformations including hypospadias in mice of the DES E12–P10 and DES P0–P10 groups. MUMP cartilage differentiation is easily detected by histology, immunohistochemistry (von der Mark, 1980; Wang et al., 2005) or by molecular techniques (Pizette and Niswander, 2001). Future studies can use the above treatment protocols and development markers in perinatally estrogen-treated mice examined at day P10, knowing that certain developmental perturbations will inevitably lead to enduring adult mouse hypospadias.

Acknowledgments

Q5 This work was supported by NIH Grant RO1 DK0581050.

References

- Agras, K., Shiroyanagi, Y., Baskin, L.S., 2007. Progesterone receptors in the developing genital tubercle: implications for the endocrine disruptor hypothesis as the etiology of hypospadias. *J. Urol.* 178, 722–727.
- Baskin, L.S., 2000. Hypospadias and urethral development. *J. Urol.* 163, 951–956.
- Baskin, L.S., Colborn, T., Himes, K., 2001a. Hypospadias and endocrine disruption: is there a connection? *Environ. Health Perspect.* 109, 1175–1183.
- Baskin, L.S., Ebbers, M.B., 2006. Hypospadias: anatomy, etiology, and technique. *J. Pediatr. Surg.* 41, 463–472.
- Baskin, L.S., Erol, A., Jegatheesan, P., Li, Y., Liu, W., Cunha, G.R., 2001b. Urethral seam formation and hypospadias. *Cell. Tissue Res.* 305, 379–387.
- Baskin, L.S., Erol, A., Li, Y.W., Cunha, G.R., 1998. Anatomical studies of hypospadias. *J. Urol.* 160, 1108–1115.
- Blaschko, S.D., Mahawong, P., Ferretti, M., Cunha, T.J., Sinclair, A., Wang, H., Schlomer, B.J., Risbridger, G., Baskin, L.S., Cunha, G.R., 2013. Analysis of the effect of estrogen/androgen perturbation on penile development in transgenic and diethylstilbestrol-treated mice. *Anat. Rec.* 296, 1127–1141.
- Bowman, C.J., Barlow, N.J., Turner, K.J., Wallace, D.G., Foster, P.M., 2003. Effects of in utero exposure to finasteride on androgen-dependent reproductive development in the male rat. *Toxicol. Sci.: Off. J. Soc. Toxicol.* 74, 393–406.
- Buchanan, D.L., Kurita, T., Taylor, J.A., Lubahn, D.L., Cunha, G.R., Cooke, P.S., 1998. Role of stromal and epithelial estrogen receptors in vaginal epithelial proliferation, stratification and cornification. *Endocrinology* 139, 4345–4352.
- Buckley, J., Willingham, E., Agras, K., Baskin, L.S., 2006. Embryonic exposure to the fungicide vinclozolin causes virilization of females and alteration of progesterone receptor expression in vivo: an experimental study in mice. *Environ. Health* 5, 4.
- Carmichael, S.L., Shaw, G.M., Laurent, C., Croughan, M.S., Olney, R.S., Lammer, E.J., 2005. Maternal progesterin intake and risk of hypospadias. *Arch. Pediatr. Adolesc. Med.* 159, 957–962.
- Clark, R.L., Anderson, C.A., Prahalada, S., Robertson, R.T., Lochry, E.A., Leonard, Y.M., Stevens, J.L., Hoberman, A.M., 1993. Critical developmental periods for effects on male rat genitalia induced by finasteride, a 5 alpha-reductase inhibitor. *Toxicol. Appl. Pharmacol.* 119, 34–40.
- Clark, R.L., Antonello, J.M., Grossman, S.J., Wise, L.D., Anderson, C., Bagdon, W.J., Prahalada, S., MacDonald, J.S., Robertson, R.T., 1990. External genitalia abnormalities in male rats exposed in utero to finasteride, a 5 alpha-reductase inhibitor. *Teratology* 42, 91–100.
- Cunha, G.R., Sinclair, A., Risbridger, G., Hutson, J., Baskin, L.S., 2015a. Current understanding of hypospadias: relevance of animal models. *Nat. Rev. Urol.* 12, 271–280.
- Cunha, G.R., Sinclair, A., Risbridger, G., Hutson, J., Baskin, L.S., 2015b. Current Understanding of Hypospadias: Relevance of Animal Models *Nature Reviews (In Press)*.
- Drey, E.A., Kang, M.S., McFarland, W., Darney, P.D., 2005. Improving the accuracy of fetal foot length to confirm gestational duration. *Obs. Gynecol.* 105, 773–778.
- Foster, P.M., Harris, M.W., 2005. Changes in androgen-mediated reproductive development in male rat offspring following exposure to a single oral dose of flutamide at different gestational ages. *Toxicol. Sci.: Off. J. Soc. Toxicol.* 85, 1024–1032.
- Gray Jr., L.E., Ostby, J.S., Kelce, W.R., 1994. Developmental effects of an environmental antiandrogen: the fungicide vinclozolin alters sex differentiation of the male rat. *Toxicol. Appl. Pharmacol.* 129, 46–52.
- Hutson, J.M., Baskin, L.S., Risbridger, G., Cunha, G.R., 2014. The power and perils of animal models with urogenital anomalies: handle with care. *J. Pediatr. Urol.* 10, 699–705.
- Hynes, P.J., Fraher, J.P., 2004a. The development of the male genitourinary system: II. The origin and formation of the urethral plate. *Br. J. Plast. Surg.* 57, 112–121.
- Hynes, P.J., Fraher, J.P., 2004b. The development of the male genitourinary system: III. The formation of the spongiosae and glandular urethra. *Br. J. Plast. Surg.* 57, 203–214.
- Iguchi, T., Uesugi, Y., Takasugi, N., Petrow, V., 1991. Quantitative analysis of the development of genital organs from the urogenital sinus of the fetal male mouse treated prenatally with a 5 alpha-reductase inhibitor. *J. Endocrinol.* 128, 395–401.
- Kalfa, N., Philibert, P., Baskin, L.S., Sultan, C., 2011. Hypospadias: interactions between environment and genetics. *Mol. Cell. Endocrinol.* 335, 89–95.
- Kim, K.S., Torres Jr., C.R., Yucel, S., Raimondo, K., Cunha, G.R., Baskin, L.S., 2004. Induction of hypospadias in a murine model by maternal exposure to synthetic estrogens. *Environ. Res.* 94, 267–275.
- Kojima, Y., Hayashi, Y., Mizuno, K., Mogami, M., Sasaki, S., Kohri, K., 2002. Spermatogenesis, fertility and sexual behavior in a hypospadiac mouse model. *J. Urol.* 167, 1532–1537.
- Lee, O.T., Durbin-Johnson, B., Kurzrock, E.A., 2013. Predictors of secondary surgery after hypospadias repair: a population based analysis of 5000 patients. *J. Urol.* 190, 251–255.
- Li, Y., Sinclair, A., Cao, M., Shen, J., Choudhry, S., Cunha, G.R., Baskin, L., 2014. Canalization of the urethral plate precedes fusion of the urethral folds during male penile urethral development: the double zipper hypothesis. *J. Urol.* 193, 1353–1359.
- Macleod, D.J., Sharpe, R.M., Welsh, M., Finken, M., Scott, H.M., Hutchison, G.R., Drake, A.J., van den Driesche, S., 2010. Androgen action in the masculinization programming window and development of male reproductive organs. *Int. J. Androl.* 33, 279–287.
- Mahawong, P., Sinclair, A., Li, Y., Schlomer, B., Rodriguez, E., Ferretti, M., Liu, B., Baskin, L.S., Cunha, G.R., 2014a. Comparative effects of neonatal diethylstilbestrol on external genitalia development in adult males of two mouse strains with differential estrogen sensitivity. *Differ. Res. Biol. Divers.* 88, 70–83.
- Mahawong, P., Sinclair, A., Li, Y., Schlomer, B., Rodriguez, E., Ferretti, M., Liu, B., Baskin, L.S., Cunha, G.R., 2014b. Prenatal diethylstilbestrol induces malformation of the external genitalia of male and female mice and persistent second-generation developmental abnormalities of the external genitalia in two mouse strains. *Differ. Res. Biol. Divers.*, In Press
- Nordenvall, A.S., Frisen, L., Nordenstrom, A., Lichtenstein, P., Nordenskjold, A., 2013. A population-based nationwide study of hypospadias in Sweden, 1973–2009: incidence and risk factors. *J. Urol.*
- Ormond, G., Nieuwenhuijsen, M.J., Nelson, P., Toledano, M.B., Iszatt, N., Geneletti, S., Elliott, P., 2009. Endocrine disruptors in the workplace, hair spray, folate supplementation, and risk of hypospadias: case-control study. *Environ. Health Perspect.* 117, 303–307.
- Ostby, J., Kelce, W.R., Lambright, C., Wolf, C.J., Mann, P., Gray Jr., L.E., 1999. The fungicide procymidone alters sexual differentiation in the male rat by acting as an androgen-receptor antagonist in vivo and in vitro. *Toxicol. Ind. Health* 15, 80–93.
- Paulozzi, L.J., 1999. International trends in rates of hypospadias and cryptorchidism. *Environ. Health Perspect.* 107, 297–302.
- Paulozzi, L.J., Erickson, J.D., Jackson, R.J., 1997. Hypospadias trends in two US surveillance systems. *Pediatrics* 100, 831–834.
- Pizette, S., Niswander, L., 2001. Early steps in limb patterning and chondrogenesis. *Novartis Found. Symp.* 232, 23–36 (discussion 36–46).
- Rider, C.V., Furr, J., Wilson, V.S., Gray Jr., L.E., 2008. A mixture of seven antiandrogens induces reproductive malformations in rats. *Int. J. Androl.* 31, 249–262.
- Rider, C.V., Wilson, V.S., Howdeshell, K.L., Hotchkiss, A.K., Furr, J.R., Lambright, C.R., Gray Jr., L.E., 2009. Cumulative effects of in utero administration of mixtures of “antiandrogens” on male rat reproductive development. *Toxicol. Pathol.* 37, 100–113.
- Rodriguez Jr., E., Weiss, D.A., Ferretti, M., Wang, H., Menshenia, J., Risbridger, G., Handelsman, D., Cunha, G., Baskin, L., 2012. Specific morphogenetic events in mouse external genitalia sex differentiation are responsive/dependent upon androgens and/or estrogens. *Differ. Res. Biol. Divers.* 84, 269–279.
- Rodriguez Jr., E., Weiss, D.A., Yang, J.H., Menshenia, J., Ferretti, M., Cunha, T.J., Barcellos, D., Chan, L.Y., Risbridger, G., Cunha, G.R., Baskin, L.S., 2011. New insights on the morphology of adult mouse penis. *Biol. Reprod.* 85, 1216–1221.
- Schlomer, B.J., Ferretti, M., Rodriguez Jr., E., Blaschko, S., Cunha, G., Baskin, L., 2013. Sexual differentiation in the male and female mouse from days 0 to 21: a detailed and novel morphometric description. *J. Urol.* 190, 1610–1617.
- Seifert, A.W., Harfe, B.D., Cohn, M.J., 2008. Cell lineage analysis demonstrates an endodermal origin of the distal urethra and perineum. *Dev. Biol.* 318, 143–152.
- Taguchi, O., Cunha, G.R., Robboy, S.J., 1983. Experimental study of the effect of diethylstilbestrol on the development of the human female reproductive tract. *Int. J. Biol. Res. Pregnancy* 4, 56–70.
- von der Mark, K., 1980. Immunological studies on collagen type transition in chondrogenesis. *Curr. Top. Dev. Biol.* 14, 199–225.
- Wang, M.H., Baskin, L.S., 2008. Endocrine disruptors, genital development and hypospadias. *J. Androl.* 29, 499–505.
- Wang, Y., Belflower, R.M., Dong, Y.F., Schwarz, E.M., O’Keefe, R.J., Drissi, H., 2005. Runx1/AML1/Cbfa2 mediates onset of mesenchymal cell differentiation toward chondrogenesis. *J. Bone Miner. Res.: Off. J. Am. Soc. Bone Miner. Res.* 20, 1624–1636.
- Welsh, M., MacLeod, D.J., Walker, M., Smith, L.B., Sharpe, R.M., 2010. Critical

- 1 androgen-sensitive periods of rat penis and clitoris development. *Int. J. Androl.* 33, e144–e152. 67
- 2 Welsh, M., Saunders, P.T., Fisker, M., Scott, H.M., Hutchison, G.R., Smith, L.B., Sharpe, 68
- 3 R.M., 2008. Identification in rats of a programming window for reproductive 69
- 4 tract masculinization, disruption of which leads to hypospadias and cryp- 70
- 5 torchidism. *J. Clin. Investig.* 118, 1479–1490. 71
- 6 Welsh, M., Saunders, P.T., Sharpe, R.M., 2007. The critical time window for andro- 72
- 7 gen-dependent development of the Wolffian duct in the rat. *Endocrinology* 73
- 8 148, 3185–3195. 74
- 9 West, N.B., Brenner, R.M., 1985. Progesterone-mediated suppression of estradiol 75
- 10 receptors in cynomolgus macaque cervix, endometrium and oviduct during 76
- 11 sequential estradiol-progesterone treatment. *J. Steroid Biochem.* 22, 29–37. 77
- 12 Willingham, E., Agras, K., de Souza Jr., A.E., Konijeti, R., Yucel, S., Rickie, W., Cunha, 78
- 13 G.R., Baskin, L.S., 2006a. Steroid receptors and mammalian penile development: 79
- 14 an unexpected role for progesterone receptor? *J. Urol.* 176, 728–733. 80
- 15 Willingham, E., Agras, K., Vilela, M., Baskin, L.S., 2006b. Loratadine exerts estrogen- 81
- 16 like effects and disrupts penile development in the mouse. *J. Urol.* 175, 82
- 17 723–726. 83
- 18 Willingham, E., Baskin, L.S., 2007. Candidate genes and their response to environ- 84
- 19 mental agents in the etiology of hypospadias. *Nat. Clin. Pr. Urol.* 4, 270–279. 85
- 20 Wilson, J.D., Griffin, J.E., Leshin, M., George, F.W., 1981. Role of gonadal hormones in 86
- 21 development of the sexual phenotypes. *Hum. Genet.* 58, 78–84. 87
- 22 Wolf Jr., C., Lambright, C., Mann, P., Price, M., Cooper, R.L., Ostby, J., LE Jr., Gray, 1999. 88
- 23 Administration of potentially antiandrogenic pesticides (procymidone, linuron, 89
- 24 iprodione, chlozolinate, p,p'-DDE, and ketoconazole) and toxic substances (di- 90
- 25 butyl- and diethylhexyl phthalate, PCB 169, and ethane dimethane sulphonate) 91
- 26 during sexual differentiation produces diverse profiles of reproductive mal- 92
- 27 formations in the male rat. *Toxicol. Ind. Health* 15, 94–118. 93
- 28 Yang, J.H., Menshenina, J., Cunha, G.R., Place, N., Baskin, L.S., 2010. Morphology of 94
- 29 mouse external genitalia: implications for a role of estrogen in sexual di- 95
- 30 morphism of the mouse genital tubercle. *J. Urol.* 184, 1604–1609. 96
- 31 Yucel, S., Cavalcanti, A.G., Desouza, A., Wang, Z., Baskin, L.S., 2003. The effect of 97
- 32 oestrogen and testosterone on the urethral seam of the developing male mouse 98
- 33 genital tubercle. *BJU Int.* 92, 1016–1021. 99
- 34 100
- 35 101
- 36 102
- 37 103
- 38 104
- 39 105
- 40 106
- 41 107
- 42 108
- 43 109
- 44 110
- 45 111
- 46 112
- 47 113
- 48 114
- 49 115
- 50 116
- 51 117
- 52 118
- 53 119
- 54 120
- 55 121
- 56 122
- 57 123
- 58 124
- 59 125
- 60 126
- 61 127
- 62 128
- 63 129
- 64 130
- 65 131
- 66 132